Research Square

Preprints are preliminary reports that have not undergone peer review.
They should not be considered conclusive, used to inform clinical practice,
or referenced by the media as validated information.

Granzyme A amplifies human neutrophil pyroptosis

Paulina Kasperkiewicz

paulina.kasperkiewicz@pwr.edu.pl

Wroclaw University of Science and Technology https://orcid.org/0000-0002-1291-047X

Aleksandra Korba-Mikołajczyk

Wroclaw University of Science and Technology

Katarzyna Służalska

Wroclaw University of Science and Technology https://orcid.org/0000-0002-6307-0204

Edyta Bielec

Wroclaw University of Science and Technology

Kornelia Steindel

Wroclaw University of Science and Technology

Ronald Piotrowski

Wroclaw University of Science and Technology https://orcid.org/0009-0007-3130-2916

Julia Miśkiewicz

Wroclaw University of Science and Technology

Melanie Brügger

University of Bern

Nedim Kozerac

University of Bern

Scott Snipas

Sanford Burnham Prebys Medical Discovery Institute

Sonia Kołt

Wroclaw University of Science and Technology

Stanisław Potoczek

Wroclaw Medical University

Jocelyn Wanjian-Tang

Genentech

Daniel Kirchhofer

Genentech

Guy Salvesen

Sanford Burnham Prebys Medical Discovery Institute https://orcid.org/0000-0002-7933-6732

Charaf Benarafa

University of Bern https://orcid.org/0000-0002-2049-7769

Article

Keywords: Granzyme A, Regulated Cell Death, Human Neutrophils, Gasdermins, Serine Protease, Pyroptosis

Posted Date: September 18th, 2026

DOI: https://doi.org/10.21203/rs.3.rs-10842867/v1

License: This work is licensed under a Creative Commons Attribution 4.0 International License. Read Full License

Additional Declarations: There is no duality of interest

Abstract

Neutrophil granule serine proteases contribute to antimicrobial defence and regulate inflammatory cell death programs. Granzyme A (GrA) expression in neutrophils is controversial and its role in neutrophil cell death remains unknown. Here, we show that pharmacological inhibition of GrA with the selective covalent inhibitor iSK15 delays and attenuates pyroptotic death induced by nigericin and granule permeabilization, while leaving spontaneous apoptosis intact. Pan-caspase inhibition was less efficient than iSK15 at inhibiting pyroptosis, suggesting that GrA amplifies pyroptotic execution through a caspase-independent mechanism downstream of inflammasome activation. GrA directly cleaved gasdermin D (GSDMD) and GSDME, but did not generate stable canonical N-terminal pore-forming fragments, indicating that GrA enhances pyroptosis via gasdermin-independent pathways. During pyroptosis, active GrA remained predominantly intracellular, relocating to the cytosol and was released from cells only at late stages, most likely as a consequence of terminal cell lysis. GrA inhibition also reduced reactive oxygen species generation. GrA-deficient mouse neutrophils did not differ from wild-type neutrophils upon nigericin stimulation, consistent with species-specific differences in GrA structure and substrate specificity. In contrast, the role of GrA was confirmed in human iPSC-derived neutrophil-like cells. Together, our findings identify GrA as a non-canonical regulator of neutrophil pyroptosis and support selective GrA inhibition as a potentially tractable strategy for modulating neutrophil-driven inflammatory responses.

Introduction

Neutrophils are the most abundant circulating leukocytes and represent a frontline component of innate immunity and are rapidly recruited to sites of infection and tissue damage. Once considered short-lived effector cells engaged primarily in microbial clearance (1), neutrophils are now recognized as central regulators of inflammation, that can shape the magnitude, duration, and resolution of immune responses through crosstalk with both innate and adaptive immune compartment (2, 3). This functional complexity demands precise control of neutrophil lifespan. When regulatory mechanisms fail, through premature elimination or pathological persistence, neutrophils drive chronic inflammation, autoimmunity, and impaired host defence (4). Decoding the molecular programs that govern neutrophil death is therefore essential for understanding immune homeostasis and for identifying therapeutic targets in neutrophil-associated disorders, including sepsis (5), neutropenia (6), and autoinflammatory disease (7).

Neutrophils can undergo multiple distinct cell death programs, each with different inflammatory consequences. Under Homeostatic conditions, the bone marrow of adult humans produces 10^{11} neutrophils per day and as many neutrophils also undergo apoptosis leading to surface expression of eat-me signals and efferocytosis by macrophages in the marrow, spleen and liver (8, 9). This inflammatory silent removal of apoptotic neutrophils also down-regulates granulopoiesis through the regulation of feedback loops (10, 11). In inflammatory conditions, neutrophil survival is prolonged via inhibition of intrinsic and extrinsic pathways of apoptosis and antimicrobial functions of neutrophils are enhanced (5). When these mechanisms are exhausted and efferocytosis is insufficient, a lytic form of

cell death ensues with the release of cellular proteins known as danger-associated molecular patterns (DAMPs), which fuel inflammatory reactions further. This lytic form of cell death referred to as neutrophil secondary necrosis is molecularly related to pyroptosis since it is mediated in part by gasdermin E (GSDME), which is activated by caspase-3 cleavage (12, 13). Cell death can also occur after the extrusion of neutrophil extracellular traps (NETs), which entrap and neutralize pathogens (14, 15). While the term NETosis is often used in the literature, the mechanisms of NET release do not necessarily involve cell death (16, 17). The relative contribution of each death program in neutrophils is highly microenvironment-dependent, shaped by the nature of the stimulus, local cytokine milieu, and the activation state of the cell (18).

Neutrophil granules are a rich source of serine proteases (NSPs), including neutrophil elastase (NE), cathepsin G (CatG), and proteinase 3 (PR3). NSPs mediate antimicrobial functions and regulate inflammatory cytokine release and function (18–22). NSPs also regulate neutrophil survival and cell death. Pathogenic mutations in ELANE, the gene encoding NE, are the most common genetic cause of severe congenital neutropenia (23). Deficiency in serine protease inhibitors (serpins) that inhibit NSPs also lead to increased neutrophil death triggered by multiple pathways (24, 25). CatG appears as the main driver of cell death in mouse neutrophils by promoting caspase-dependent and independent pathways (26). The release of CatG into the cytosol induces neutrophil death (25). Conversely, NE has been implicated in driving NETosis by mediating GSDMD cleavage and promoting nuclear membrane pore formation and DNA release. Given the propensity of gasdermins to be activated by cleavage, we reasoned that other granule-resident proteases may similarly engage gasdermin family members. Of particular interest is Granzyme A (GrA), which belongs to a family of proteases structurally and mechanistically related to NSPs, but with distinct substrate specificities (27). Granzyme A (GrA) is a trypsin-like serine protease classically associated with cytotoxic lymphocyte-mediated killing and has been recently identified in neutrophil granules (28). This finding was initially disputed (29) but subsequently confirmed by multiple independent methods including flow cytometry, western blot, and subcellular fractionation (28). Its functional role in neutrophil biology nonetheless remains poorly characterized. In cytotoxic lymphocytes, GrA induces perforin-dependent but caspase-independent death of target cells by disrupting mitochondrial function, generating reactive oxygen species (ROS), and causing single-stranded DNA damage (30, 31). Whether GrA contributes to neutrophil cell death, and by what mechanism, has not been defined. Accordingly, we set out to investigate potential roles for GrA in paradigms of cell death, using a multi-model approach encompassing primary human neutrophils, GrA-deficient murine neutrophils, neutrophils differentiated from induced human pluripotent stem cells (iPSC-neu). In addition, we used the tool compound iSK15 (Fig. 1A), a selective, covalent inhibitor of GrA (32) to test the hypothesis that cleavage of gasdermins would drive forward a pyroptotic phenotype.

Materials and methods

Human Neutrophils Isolation

The collection of peripheral blood from healthy adult volunteers was approved by the Local Bioethics Committee at the Medical University of Wrocław (KB 326/2022). Peripheral blood was obtained from healthy adult donors (18–70 years of age) of both sexes, whose eligibility was confirmed by a medical interview. Blood samples were collected into EDTA-coated Vacutainer tubes. Neutrophil isolation was performed within 2 hours (h) of blood collection. When required, samples were diluted with calcium- and magnesium-free Dulbecco's phosphate-buffered saline (DPBS, Gibco). Granulocytes were isolated by density gradient centrifugation using Polymorphprep (Progen) and Ficoll-Paque (Cytiva) as previously described in [33]. Specifically, 1 mL of Ficoll-Paque was carefully layered over 4 mL of Polymorphprep, followed by 5 mL of EDTA blood. Samples were centrifuged at 450 × g for 35 minutes (min) at room temperature with no brakes. The granulocyte-rich layer was collected, diluted with HBSS (Gibco) containing 15 mM EDTA (HBSS/EDTA, Invitrogen) to a final volume of 50 mL, and centrifuged at 250 × g for 5 min. Residual erythrocytes were lysed in ammonium chloride lysis buffer (168 mM NH_4Cl, 10 mM EDTA, 12 mM $NaHCO_3$, pH 7.3) or a commercial solution (BioLegend) on ice for 10 min followed by washing in HBSS/EDTA. The procedure was repeated once if necessary. Purified granulocytes were resuspended in complete RPMI-1640 medium without phenol red and supplemented with 10% FBS (Gibco), 100 U/mL penicillin/streptomycin (LifeTechnologies) and 2 mM glutamine (Sigma-Aldrich). Cell counts and viability (> 95%) were determined using Trypan Blue and Invitrogen Countess 3 automated cell counter. The statistical analysis was prepared from 3 experiments, each performed on cells isolated from different, individual volunteer.

Mouse Neutrophils Isolation

Mice were maintained in individually ventilated cages (Tecniplast), with 12h/12h light/dark cycle, 22 ± 1°C ambient temperature and 50 ± 20% humidity, autoclaved food and acidified water. Mouse neutrophils were isolated from the bone marrow of C57BL/6J (WT) and granzyme A-deficient ($GrA^{-/-}$) male and female mice. $GrA^{-/-}$ mice (B6.Cg-*Gzma*^{tm1Simn}) were originally generated using C57BL/6 ES cells and were rederived from frozen embryos obtained from the Australian Phenome Facility. The mice were further backcrossed to C57BL/6J mice for at least 5 more generations at the IVI. Following euthanasia with CO_2, femurs and tibias were dissected under sterile conditions and flushed with ice-cold flushing medium (DPBS, 0.5% FBS, 0.5 x Penicillin/Streptomycin, 2 mM EDTA). The cell suspension was filtered through a 70 μm cell strainer and centrifuged at 350 × g for 10 min at 4°C, resuspended in 10 mL of 1× RBC lysis Buffer (150 mM NH_4Cl, 10 mM $NaHCO_3$, 1 mM EDTA) and incubated on ice for 10 min to lyse erythrocytes. The reaction was stopped by adding at least twice the volume of flushing medium, followed by centrifugation at 350 × g for 10 min.

Neutrophil isolation was performed by positive selection using magnetic-activated cell sorting (MACS, MidiMACS™ separator, Miltenyi Biotec) with anti-Ly-6G MicroBeads (Miltenyi Biotec, Cat# 130-120-337) following the manufacturer's instructions. Cells were counted using the LUNA-Fx7™ automated cell counter with acridine orange to distinguish live and dead cells. Precise cell counts were determined by averaging three counts and cells were suspended in complete RPMI-1640 supplemented with 10% FBS,

50 µM β-mercaptoethanol, 10 mM HEPES and 2mM Glutamax (ThermoFisher). Statistical analyses were performed from 3 independent experiments, each conducted with neutrophils isolated from different mice.

Cell Culture of Cell Lines

All cell lines used were human-derived and obtained from commercial sources (ATCC, DSMZ, Synthego) and cultured in a Biosafety Level 2 (BSL-2) laboratory under sterile conditions. NK92 cells were maintained in α-MEM (Gibco) supplemented with 12.5% horse serum (Sigma-Aldrich) and 50 U/mL interleukin-2 (Pepro-Tech). HeLa cells were grown in DMEM (Sigma-Aldrich) supplemented with 10% FBS and 100 U/mL of penicillin and streptomycin. HEK293T cells (generous gift from Prof. Guy Salvesen) were grown in DMEM supplemented with 10% FBS and 100 U/mL of penicillin and streptomycin, additionally the adherent cells were detached prior to passaging for 5 min, at 37°C using TrypLE Express Enzyme solution (Gibco). Cells were cultured in a humified 5% CO_2 atmosphere at 37°C with and passaged every 2–3 days at maximum density. For passaging, cells were centrifuged at 400 × g for 5 min, resuspended in fresh medium, and returned to incubation. iPS cells were seeded and cultured at a density of 1×10^6 cells, resuspended in 1.5 mL of medium per well. Essential 8 medium (Gibco) supplemented with 1 µg/mL of heparin (Sigma-Aldrich) without antibiotics in 6-well plates precoated for 1h in 37°C with Geltrex (Gibco) diluted 1:100 with prechilled DMEM/F12 medium (Gibco). iPS cells were passaged at 80–90% confluency using 0.5 mM EDTA solution (Invitrogen) in DPBS and centrifuged at 150 × g for 3 min. After thawing or passaging medium was additionally supplemented with 10 µM Y-27632 dihydrochloride (Tocris). Medium was exchanged daily. Cell counts and viability were determined using an Invitrogen Countess 3 cell counter (Thermo Fisher Scientific) and Trypan Blue. Cells used for the experiments obtained viability > 95%.

Induction of Neutrophil Cell Death

Human neutrophils

Freshly isolated neutrophils were seeded at a density of 1×10^6 cells in 1 mL of medium, per well of a 6-well plate (Corning) pre-treated for cell adhesion. Cells were incubated in phenol red-free RPMI-1640 medium with 10% FBS (Gibco), 100 U/mL penicillin/streptomycin (LifeTechnologies), and 2 mM glutamine. To inhibit GrA, neutrophils were pre-incubated for 1 h at 37°C and 5% CO_2 with 500 nM iSK15 (selective granzyme A inhibitor). The synthesis of iSK15 and its kinetic parameters have been described previously (32). Cell Death was subsequently induced by treatment with 10 µM nigericin for 4 h. For selected experiments, neutrophils were primed with 1 µg/mL LPS (Sigma-Aldrich) for 3 h at 37°C and 5% CO_2, followed by stimulation with 10 µM nigericin for 1 h to enhance pyroptosis. Untreated cells served as controls. Cells and culture supernatants were then analyzed by flow cytometry or collected for biochemical assays, respectively.

Mouse neutrophils

Positively selected WT and GrA$^{-/-}$ mouse neutrophils (1 × 10⁶ cells/well) were seeded in 6-well plates in complete RPMI-1640. Neutrophils were incubated with 15 μM nigericin (Sigma-Aldrich) for 0, 4, 6 and 18 h at 37°C and 5% CO_2. Cell death was analyzed by flow cytometry based on FSC/SSC profile and 7-AAD (BioLegend) staining. Data acquisition was performed using a BD FACS Canto and the data was analyzed using FlowJo v10.10.

iPS Cells Differentiation into Neutrophils

Neutrophils were generated from human iPSCs (iPSneu) using embryoid body (EB) based differentiation protocols adapted from previously published studies (33, 34). Prior to differentiation, the iPSCs were adjusted to single cells passaging using a modified method from Cruvinel et al. (35). Briefly, 1 × 10^6 cells were carefully thawed to not disturb compacted colonies and seeded, then after each passage were diluted to gradually increase the split ratio (1:4, 1:6, 1:10). Such prepared cells could be stored in the vapor phase of liquid nitrogen for further use in differentiation protocol. Viable and adjusted iPSCs were dissociated using 0.5 mM EDTA, centrifuged and resuspended in Essential 8 medium supplemented with 1 μg/mL of heparin and 10 ng/mL of FGF-basic (PeproTech) and 3 × 10^4 cells were seeded per well in BIOFLOAT 384 U-bottom well plates (faCellitate). After 2 days, EBs were collected, and then resuspended in STEMdiff Apel 2 Medium (StemCell Technologies) supplemented with 25 ng/mL interleukin-3 (PeproTech) and 50 ng/mL G-CSF (PeproTech), approximately 20 EBs (per well) were transferred to 6-well plate precoated with 1:100 diluted Geltrex. The plates were incubated without disturbing for at least 10 days to allow EBs attachment and development of myeloid cell forming complex (MCFC), which later were releasing hematopoietic progenitor cells into the culture medium. If EBs were not fully attached, the medium was replaced to fresh, and plates were incubated for an additional 7 days. Then, every 7 days for at least 3 months shed cells were collected and filtered through 100 μm cell strainer (Corning) to obtain a uniform single-cell suspension. Cells were centrifuged at 800 × g for 20 min (ac/dc 0) and resuspended into terminal differentiation medium, which was RPMI 1640 medium supplemented with 10% FBS and 100 ng/mL G-CSF, and cultured for 7 days to obtain mature neutrophils. The level of differentiation into neutrophils was assessed by flow cytometry (Supplementary Figure S3). The schematic representation of the differentiation process was presented in Supplementary Figure S3E.

Human Granzyme A ELISA

The human granzyme A ELISA (Thermo Fisher Scientific) was performed according to the manufacturer's instructions. Briefly, 96-well plates pre-coated with anti-human granzyme A were washed twice, and a seven-point granzyme A standard curve and samples, diluted in the proportion of 1:2 in sample diluent, were added in duplicate, 50 μL sample + 50 μL diluent per well. After addition of 50 μL biotin-conjugated anti-GrA to all wells, plates were incubated for 2 h at room temperature (18–25°C) on a

microplate shaker, followed by four washes and a 1 h incubation with streptavidin–HRP, 100 µL/well, under the same conditions. Plates were then washed four times, developed with 100 µL TMB substrate for 30 min at room temperature, and the reaction was stopped with 100 µL stop solution; absorbance was read at 450 nm, and granzyme A concentrations were calculated from the standard curve, taking the 1:2 sample dilution into account. The data was analysed based on duplicates from n = 3, where each n was an experiment performed from neutrophils isolated from three healthy individuals.

Live-Cell Imaging of Neutrophil Cell Death and ROS Formation in Neutrophils

Freshly isolated neutrophils were seeded at a density of 1×10^5 cells per well in µ-Slide 18-well plates (Ibidi). Controls were untreated, while granzyme A inhibition involved neutrophil pre-incubation for 1 h at 37°C, 5% CO_2 with either 500 nM iSK15 or Nafamostat mesylate (Sigma-Aldrich). Afterwards, cell death was induced as described in the previous section. For live/dead cell distinction, SYTOX™ Green (Invitrogen) at final concentration of 1 µM was added per well. ROS detection was carried out by adding 5 µM CellROX (Invitrogen) to each well and live-cell imaging lasted 2 h. Imaging was conducted on a Leica DMi8 inverted confocal microscope with a 63×/1.40–0.60 oil immersion lens. Over 4 h, images were acquired every 30 min (cell death) or 10 min (ROS) in two channels (brightfield, and fluorescence) with Z-stack acquisition. Cells were excited at 488 nm. Image acquisition/experiment control used LAS X Leica software; live/dead cell ratio quantification and statistical analysis (with normalization) were conducted in LAS X Leica and GraphPad Prism software, respectively.

Flow Cytometry Analysis of Neutrophil Viability and ROS Production in Neutrophils

Neutrophils were prepared and treated as described in the above. Samples were collected at 0, 1, 2, 4 h of incubation for neutrophil viability assay, and at 0, 10, 20-, 30-, 60-, and 120-min post-induction for ROS production assay. Cells were centrifuged at 250 × g for 5 min at 4°C. 900 µL of supernatant was removed, and cells were resuspended in the remaining 100 µL medium. For assessment of neutrophil viability, 1 µM SYTOX Green (Invitrogen) was used, while for the analysis of ROS production 5 µM CellROX (Invitrogen) was added to each sample. Measurements were performed on a CellStream (Amnis) flow cytometer, acquiring 10,000 single-cell events per sample. Granulocytes were identified by side scatter (SSC) and forward scatter (FSC), live/dead and ROS-positive cells were gated by CellROX fluorescence at 488 nm and SSC. Data was visualized as histograms and analysed in FlowJo v10.10.

SDS-PAGE and Western blot Analysis

SDS-PAGE was performed with 1 mm-thick Bolt™ 4–12% Bis-Tris gradient gels (Invitrogen) or home-made 10% acrylamide gels. Protein samples were denatured in 1× SDS sample buffer (187.5 mM Tris-HCl, pH 6.8, 6% SDS, 30% glycerol, 0.03% bromophenol blue, 20% DTT), at 95°C for 5 min, then centrifuged at 12,400 × g for 5 min and 10 µL was poured onto gel. Electrophoresis was run at 165 V for 35 min at room temperature in 1× Bolt™ MES SDS Running Buffer (Invitrogen) using a Mini Gel Tank

(Invitrogen) and PowerPac HC power supply (Bio-Rad). PageRuler Plus Prestained Protein Ladder (Thermo Scientific) was used for molecular weight determination. Proteins were transferred to 0.2 µm nitrocellulose membranes (Bio-Rad) via wet transfer in a Mini Blot Module (Invitrogen™) with 1× Bolt™ Transfer Buffer, at 10 V for 60 min. Transfer efficiency was verified by Ponceau S staining (0.1% Ponceau S, 1% glacial acetic acid). Membranes were washed with TBS-T (Tris-buffered saline, 0.1% Tween-20) and blocked for 60 min at room temperature with 5% BSA (Sigma-Aldrich) in TBS-T. Primary antibodies were diluted in TBS-T with 3% BSA (Sigma-Aldrich) according to manufacturer's requirements, a list of all primary and secondary antibodies used is presented in table 1. Membranes were subjected to incubation with primary antibodies overnight, in 4°C shaking. Membranes were washed 3 times with TBS-T for 5 mins, rocking. Membranes were incubated with secondary antibodies, as suggested by the manufacturer in TBS-T with 3% BSA in RT, for 1 h. Proteins were detected and visualized with a Sapphire Biomolecular Imager (Azure) using 658 nm and 488 nm lasers.

Detection and Inhibition Assay of Granzyme A in Neutrophil Lysates

Inhibitor (iSK15) and activity-based probe (SK15.5) specificity and working concentrations were validated as previously described (32). For GrA detection in neutrophils from healthy donors, cells were lysed in 100 µL of buffer (25 mM KCl, 5 mM $MgCl_2$, 10 mM Tris-HCl, 0.5% Tween-20, pH 8.0) at a density of 1 × 10^7 cells/mL, sonicated (Bueno Biotech, 20 kHz, 10 s), and stored at − 80°C. For inhibition assays, 10 µL lysate was combined with 10 µL GrA buffer (50 mM Tris, 100 mM NaCl, 5 mM $CaCl_2$, 0.01% Tween-20, pH 7.5) and iSK15 at final concentrations of 0–600 nM, or buffer as controls. After 1 h at 37°C, 5 µL of activity-based probe (SK15.5) specific for GrA (final 500 nM) was added, followed by a further 1 h incubation at 37°C. Reactions were terminated by the addition of 3 × SDS sample buffer containing 20% DTT, then heated to 95°C for 5 min, and centrifuged at 12,400 × g for 5 min. Samples were subjected to SDS-PAGE and Western blotting. GrA was detected using an anti-GrA antibody and fluorescent secondary antibody (excitation: 658 nm and 488 nm), described in Table 1. NK92 cell lysates served as positive controls.

For the detection of murine GrA, neutrophils were isolated as described above and 1 × 10^6 cells/mL cells per sample, lysed using 100 µL RIPA buffer (Sigma-Aldrich). Both NK92 cell lysates and human neutrophil lysates served as controls. The western blotting was performed the same way as for human samples. GrA and NE activity-based probes were visualized using Azure Sapphire (excitation 649 nm).

Detection and Localization of Granzyme A in Neutrophil Granules

Confocal slides (Superfrost, Epredia) were prepared with three hydrophobic pen-defined circular fields, each receiving 40 µL Poly-D-lysine (Gibco) and incubated for 1 h at room temperature, then washed twice with nuclease-free water, air-dried for 30 min. Neutrophils (3 × 10^4 cells/field) were seeded in 40 µL RPMI-1640 medium with 10% FBS, 100 U/mL penicillin/streptomycin, and 2 mM glutamine, incubated 1 h at 37°C/5% CO_2. Slides were washed twice with 40 µL DPBS (Gibco), 0.5% BSA (Sigma-Aldrich), 0.2%

Triton X-100 (Sigma-Aldrich). Cells were fixed with 4% paraformaldehyde (Sigma-Aldrich) for 15 min (dark, room temperature), then washed three times with DPBS. Permeabilization used 20 µL DPBS with 0.5% BSA, 0.05% Triton X-100 for 10 min; slides were then washed twice with DPBS. Blocking was performed with 5% BSA in DPBS for 30 min. Primary antibodies were paired per circular field for protein colocalization, applied at 1:500, incubated overnight at 4°C (dark). Slides were washed three times with DPBS + 0.5% BSA, then incubated with secondary antibodies in proportion 1:500, 1 h, dark and washed again. Nuclear staining used Hoechst (Thermo Fisher Scientific) 1:1000 for 10 min, with two washes in DPBS (0.5% BSA). Slides were mounted with Fluoromount G (Sigma-Aldrich), dried 1 h under cover, and sealed with nail polish. All fluorescent steps were done in low light. Sample integrity was maintained with careful handling.

Immunofluorescence Staining of Neutrophils on Poly-D-Lysine-Coated Slides for Granzyme A Detection and Colocalization of Human Granzyme A with GSDMD and GSDME

Slides were coated with poly-D-lysine (sigma-Aldrich) and incubated for 1 h at room temperature, then washed twice with nuclease-free water, and air-dried for 30 min. Neutrophils were seeded at 3×10^4 cells per field in complete RPMI-1640 medium without phenol red and incubated for 1 h at 37°C and 5% CO_2. After medium removal, slides were washed twice with DPBS (Gibco) containing 0.5% BSA (Sigma-Aldrich) and 0.2% Triton X-100 (Sigma-Aldrich). Cells were fixed with 4% paraformaldehyde (Sigma-Aldrich) for 15 min (dark, room temperature), washed three times, and permeabilized with 20 µL permeabilization buffer (DPBS with 0.5% BSA, 0.05% Triton X-100) for 10 min, followed by two washes. Blocking was performed with 5% BSA (Sigma-Aldrich) in DPBS for 30 min. For pore-forming protein colocalization anti-GSDMD and anti-GSDME. Each antibody was used in 1:500 dilution in an antibody buffer (DPBS with 3% BSA) and incubated overnight at 4°C in the dark. After three washes in DPBS containing 0.5% BSA, slides were incubated with secondary antibodies, 1:500 dilution, 1 h, room temperature, dark. Slides were washed with DPBS/washing buffer, nuclei were counterstained with Hoechst (1:1000, ThermoFisher Scientific) for 10 min, followed by two additional washes. Slides were mounted with Fluoromount G (Sigma-Aldrich), left to dry for 1 h, and sealed with nail polish. All fluorescent steps were performed under low light to minimize photobleaching.

Immunofluorescence Staining of Neutrophils During Nigericin and LLME Induction to Localise Granzyme A

Neutrophils were isolated from three, healthy individuals as previously described. Nigericin (10 µM) and LLME (100 µM) were added to the cells for 1 h (Nigericin) and two h (LLME), prior to washing and fixation. Hoechst was used to nuclei staining and Granzyme A antibody was used to localise GrA in cells during cell death, overnight. Slides were prepared as previously described.

qPCR

Total RNA was isolated from freshly isolated neutrophils (1×10^6 cells) using TRIzol Reagent (ABP Bioscience) per the manufacturer's guidelines. cDNA was synthesized from 1 µg RNA using the High-

Capacity cDNA Reverse Transcription Kit (Thermo Fisher Scientific). qPCR was carried out with SYBR Green qPCR Premix (EurX) and custom-synthesized primers (Genomed, 200 nM; Forward: CCACACGCGAAGGTGACCTTAA, Reverse: CCTGCAACTTGGCACATGGTTC) in technical triplicates, using 20 µL reaction volumes and a 1:10 cDNA template dilution. The thermal cycling conditions were as follows: 95°C for 2 min, followed by 40 cycles of 95°C for 5 s, and 60°C for 30 s, followed by melt curve analysis. Reactions were run on a CFX Opus real-time PCR system (Bio-Rad) and data were acquired with CFX Maestro Software (Bio-Rad). Relative expression was calculated by the $2^{-\Delta Ct}$ method.

Recombinant Human Granzyme A Expression in Komagataella phaffii

Recombinant human GrA was produced using the methylotrophic yeast *Komagataella phaffii* (formerly *Pichia pastoris*) expression system. The coding sequence of human GrA was cloned into the pPIC9 expression vector under the control of the methanol-inducible AOX1 promoter. The resulting construct was transformed into the *K. phaffii* GS115 strain, and transformants were selected according to standard protocols established for this expression system. Expression clones were kindly provided by Prof. Niels Bovenschen (Utrecht University). The recombinant GrA was expressed as a secreted protein using the *Saccharomyces cerevisiae* α-mating factor (α-MF) prepro secretion signal resulting in secretion of mature recombinant GrA into the culture medium. To improve recombinant GrA production, expression conditions were optimized using a mixed-feeding strategy consisting of methanol and sorbitol at different concentrations during the induction phase. Methanol served as the inducer of the AOX1 promoter, whereas sorbitol was supplied at different concentrations as an additional non-repressing carbon source to support cellular metabolism and reduce metabolic stress during protein production as was mentioned previously increased yield of protein expression in some cases (36).

Selected transformants were initially inoculated from glycerol stocks in YPD culture medium consisted of 1% (w/v) yeast extract (Sigma Aldrich), 2% (w/v) peptone (Sigma Aldrich) and 2% (w/v) glucose (Sigma Aldrich). For preculture (not induced medium) *K. phaffii* with GrA expression vector was inoculated in 4 flasks of 200 mL, 50 mL medium per flask and cultured for 2 days in shaking incubator at 30°C, 170 rpm to generate biomass (preculture). Next, yeast density was measured using spectrophotometer (BioPhotometer D30, Eppendorf) in 1.5 ml disposable cuvette (Brand) and preculture was centrifuged in sterile bottles for 10 min at 3000 rcf (Rotina 420R, Hettich), supernatant was discarded and biomass was diluted to OD_{600}=10 in sterile buffered induction medium consisted of 1% (w/v) yeast extract (Sigma Aldrich), 2% (w/v) peptone (Sigma Aldrich), 100 mM potassium phosphate at pH 6.0 (Gibco), 1% (w/v) D- sorbitol (Sigma Aldrich), 0.1%(w/v) methanol (Chempur). Diluted cultures for recombinant protein production were split to 6 X 2L flasks, approx. 330 mL per flask. Yeast cultures were fed with methanol and sorbitol every 24 h for 5 days (3,3 mL of sterile 100% (w/v) D-sorbitol and 330 µl of 100% methanol) and cultured in shaking incubator at 30°C, 170 rpm. Samples from initial and induced yeast cultures were collected and visually examined daily using optical microscopy to eliminate contamination in fermentation media. Following induction, the conditioned medium was subjected to purification steps.

Purification of recombinant human granzyme A

Purification of recombinant human GrA was performed according to Bovenschen et al. with modifications (37). Culture supernatants (~ 2L) were collected and initially centrifuged for 20 min at 3000 rcf, 4°C to separate the biomass from the conditioned medium, and the clarified supernatant was filtered using Vacuum Filtration System (VWR) with 0,2 µm pores size. Clarified culture supernatant was diluted with dH_2O (~ 2L) to balance conductivity equivalent to equilibration buffer (50 mM MES pH 6, 50 mM NaCl) for proper protein binding. The purification was conducted using cation-exchange column (HiTrap SP FF, Cytiva) under buffer conditions that promoted binding of the positively charged GrA molecule. The column was washed with volumes recommended by manufacturers' instructions and loaded with recombinant GrA overnight in cold room (4°C) at 1 mL/minute rate using a chromatographic procedure on NGC Liquid Chromatography System (Bio-Rad Laboratories) (Supplementary Figure S5B). The column was washed with a wash buffer (50 mM MES pH 6, 100 mM NaCl) until absorbance at 280 nm on detector reached 0. Then 4 mL of elution buffer (50 mM MES pH 6, 1 M NaCl) was applied to the column, then the pump was stopped and the column was incubated with an elution buffer for 15 min to allow elution. Next, an elution buffer was applied at 1 mL/minute rate and fractions of 1 mL were collected. Protein-containing fractions were subsequently pooled then purified recombinant GrA was subjected to concentration and dialysis using Amicon Ultra Centrifugal Filter, 3 kDa MWCO columns (Millipore). The protein was dialyzed against 20 mM Tris-HCl, 150 mM NaCl (pH 7.4). Protein concentration was determined using a µCuvette® G1.0 adapter (Eppendorf) for spectrophotometer. The purified protein was supplemented with 10% (v/v) glycerol, aliquoted, and stored at − 80°C until further use. Protein purity and integrity were assessed by SDS-PAGE followed by Coomassie Brilliant Blue (InstantBlue, Abcam) staining (Supplementary Figure S5A). Enzymatic activity of recombinant GrA was confirmed by hydrolysis of the specific substrate SK17 as well as titration of active sites to determine concentration of enzyme.

Analysis of Hydrolysis of PFP by Recombinant Neutrophil Serine Proteases

Transfection vectors pcDNA3.1(+) encoding genes for human GSDME, GSDMB and NINJ1 were ordered as a custom gene synthesis (GeneUniversal, USA). HeLa cells were transiently transfected with these plasmids using Lipofectamine 3000 (Thermo Fisher Scientific) according to the manufacturer protocol. Briefly, cells were seeded onto plates 24 h before transfection, the next day 1 µg DNA was mixed with Lipofectamine 3000 in the ratio 1:3, and Power 3000 reagent, combined mixture was incubated for 15 min at room temperature and added to cells. 48 h after transfection cells were lysed in RIPA buffer (Sigma-Aldrich). In all cases, expressions of GSDME, GSDMB and NINJ1 were verified by SDS-PAGE and Western blot.

Recombinant human GrA (in-house expression) and other granzymes (GrB, GrK, GrM) were generously provided by Phillip Bird.). Purified human NE, CatG, and PR3 were from Athens Research & Technology. Neutrophil serine protease 4 (NSP4) was expressed and purified as described previously(38). For

hydrolysis studies, HEK293T and HeLa lysates were incubated with 100 nM protease at 37°C for up to 8 h. Reactions were terminated with a 3× SDS sample buffer. Hydrolysis was assessed by SDS-PAGE and Western blotting for GSDMD, GSDME, GSDMB, and NINJ1 using antibodies listed in Table 1.

Synthesis of Internally Quenched Fluorogenic (IQF) GSDMD- and GSDME-based substrates

Peptides were synthesized manually by solid-phase peptide synthesis (SPPS) using the platform previously developed in our laboratory (39). For the synthesis of each substrate, 100 mg (0.062 mmol) of Fmoc-Rink Amide AMresin with a substitution level of 0.62 mmol/g was used. The resin was placed in cartridge wells and swollen in dichloromethane (DCM) for 30 min at room temperature, with gentle stirring every 5 min. The DCM was removed via vacuum aspiration, and the resin was washed three times with *N,N*-dimethylformamide (DMF). The Fmoc group was removed using a 20% solution of piperidine in DMF in two consecutive steps (5 and 20 min), with four and six DMF washing cycles after the first and second deprotection steps respectively. Three equivalents (0.186 mmol) of Fmoc-Lys(Dnp)-OH, previously preactivated for 5 min with equimolar amounts of HOBt and DIC in 1 mL of DMF, were added to the resin. The coupling reaction was carried out for 1.5 h at room temperature with gentle agitation to ensure constant contact between the resin and the reaction solution. After the coupling was completed, the resin was washed three times with DMF, and then the Fmoc group was removed as described above. Peptide elongation was carried out following the same strategy until the target octapeptide sequence was obtained and flanked with Lys(Dnp). Three equivalent of Fmoc-ACC-OH, prepared in-house according to the procedure described by Maly et al. (40), were added; the fluorophore was preactivated in the same manner as the Fmoc-amino acids, and the reaction was carried out for 16 h at room temperature. The resin was washed three times with DMF, and the reaction was repeated using 1.5 equivalent of the same reagents for an additional 8 h. The terminal Fmoc group was then removed according to the previously described protocol. The resin was washed sequentially with DMF (6x), DCM (3x), and methanol (3x) and dried for 12 h over P_2O_5. The IQF substrates were cleaved from the resin using a mixture of trifluoroacetic acid, triisopropylsilane and water (TFA/TIPS/H_2O; 95:2,5:2,5, v/v/v). To each resin-containing well, 2 mL of the cleavage mixture was added and mixed gently once per 10 min for 2 h (room temperature). The resulting solutions containing peptides were transferred to Falcon tubes, followed by addition of cold diethyl ether and incubation for 30 min at -20^{o}C. Next the samples with yellow precipitate were centrifuged for 5 min at 4.4 x 10^3 RPM, the supernatant was removed, and precipitate was washed with 4mL Et_2O portions and spun down. All crude substrates were purified by preparative high-performance liquid chromatography in a reversed-phase system (RP-HPLC) using a Waters system (M600 solvent delivery module and M2489 detector) equipped with a preparative Discovery 10 µm C8 column. Compound purity and molecular mass were confirmed by LC-MS (Shimadzu LCMS-2050 with Phenomenex Aeris 3,6 µm XB-C18 column). The purity of the compounds was over 93%.

Kinetic Assay

All kinetic experiments were performed using a spectrofluorometer (Molecular Devices SpectraMax Gemini XPS) on 384-well, white, flat bottom, nontreated plates (Corning). The GrA assay buffer contained 50 mM Tris, 100 mM NaCl, 5 mM $CaCl_2$, 0.01% (v/v) Tween-20, pH 7.5. Buffer was prepared at room temperature prior to analysis, and the enzyme kinetic studies were performed at 37°C. The GrA enzyme used in this study was produced and purified in-house. GrA was preincubated in an assay buffer for 10 min at 37°C before being added to the wells. Each assay was performed in three replicates, and the data represent the average of these repetitions. The obtained results were analysed using SoftMax (Molecular Devices) and GraphPad Prism software.

Screening of Internally Quenched Fluorogenic (IQF) Substrates

Activity of GrA toward IQF substrates was measured as follows: 49.5 µL of GrA (final concentration 39.7 nM) was preincubated in assay buffer (50 mM Tris, 100 mM NaCl, 5 mM $CaCl_2$, 0.01% (v/v) Tween-20, pH 7.5) for 10 min at 37°C and then added to 384-well Corning plates containing 0.5 µL of substrate in each well. The final concentration of IQF substrates was 10 µM, while the reference substrate was used at a final concentration of 200 µM. Fluorescence emission was measured for at least 30 min, and the linear portion of each progress curve was used to calculate RFU/s. The excitation wavelength was 355 nm, and the emission wavelength was 460 nm. Each compound was analysed in three replicates, and the data are presented as mean ± SD.

Statistical Analysis

Statistical analyses were performed using GraphPad Prism version 10 (GraphPad Software, San Diego, CA). Data are presented as mean ± SD. Comparisons between groups across multiple time points were performed using two-way analysis of variance (ANOVA) with Šídák's multiple comparisons test. For live-cell imaging quantification, cell death and ROS data were expressed as a fraction of total cells per field and normalized to the baseline timepoint prior to statistical analysis. Pearson's correlation coefficients for colocalization analysis were calculated using LAS X software (Leica Microsystems) from a minimum of 100 cells per condition per experiment. A p-value < 0.05 was considered statistically significant (****p < 0.0001; ***p < 0.001; **p < 0.01; *p < 0.05). For human experiments, each n was a healthy and individual volunteer, for murine experiments each mouse for an individual n, with n = 3 being three individual mice, male and female per genotype. For murine FACS analysis with antibodies, three separate experiments were performed per gender and genotype.

Results

Granzyme A is stored in active form in the primary granules of human neutrophils

Whether GrA is expressed in human neutrophils has been debated previously (28, 29). Furthermore, where expression was confirmed, GrA was reported to localize to peroxidase-negative secondary and

tertiary granules rather than primary (azurophil) granules, where other NSPs are stored (41). This prompted us to perform dual immunofluorescence staining on freshly isolated human neutrophils using antibodies against GrA and established markers of primary, secondary, and tertiary granules. Quantitative colocalization analysis of over 100 cells per condition yielded high Pearson's correlation coefficients (r) between GrA and the primary granule proteases NE and PR3, while substantially lower values were obtained with the secondary granule marker lactoferrin and the tertiary granule marker MMP9 (Fig. 1B, C). In addition, RT-qPCR analysis revealed low but detectable levels of GZMA transcripts in the analyzed human peripheral blood neutrophil samples (Supplementary Fig. S2A, B). These data demonstrate that GrA shows preferential co-distribution with other primary granule serine proteases, which are expressed early in myelopoiesis with low mRNA transcript levels in mature blood neutrophils.

We next asked whether GrA is stored in catalytically active form, as reported for other granzymes and NSPs (42). To address this, we employed chemical tools based on the peptide-based substrate SK15, including the inhibitor (iSK15) and the activity-based probe (ABP) (SK15.5), which selectively labels active GrA through covalent binding to the catalytic serine (32) (Fig. 1A). Freshly isolated neutrophil lysates were incubated with increasing concentrations of iSK15 and then with an excess of the SK15.5 ABP. Lysates were separated by SDS-PAGE and proteins were transferred into nitrocellulose for fluorescence detection of total and active GrA. The anti-GrA antibody detected protein across all conditions, confirming that iSK15 treatment did not affect GrA protein levels. ABP labelling was detected in the absence and at low iSK15 concentrations, with complete inhibition achieved at 250 nM (Fig. 1D, E). Together, these findings demonstrate that GrA is constitutively present in a catalytically active form in the primary granules of human neutrophils.

GrA activity drives nigericin-induced neutrophil death independently of caspases

We first evaluated the contribution of GrA in neutrophil pyroptosis. Freshly isolated human neutrophils were pre-treated for 1 h with the GrA inhibitor iSK15, prior to stimulation with nigericin, a potent K+ ionophore. Cell death progression was monitored over 4 h by live-cell confocal imaging with SYTOX Green. iSK15 was well tolerated in the absence of nigericin, with cell viability indistinguishable from naïve untreated neutrophils throughout the imaging period. Nigericin induced rapid and progressive neutrophil death with a dense nuclear DNA staining detectable from 30 min and diffuse DNA staining after 1 h, with all cells positive with diffuse staining by 4h. In individual cells, the appearance of dense nuclear DNA staining preceded the diffuse DNA staining (Fig. 2A). This is consistent with the stepwise execution of lytic pyroptotic death, where the SYTOX dye enters the cells via gasdermin pores and subsequent mechanisms lead to nuclear and plasma membrane rupture. Pre-treatment with iSK15 substantially delayed and reduced death at all time points (Fig. 2B, C). Importantly, iSK15 completely suppressed early nuclear DNA staining and delayed the onset of cell lysis (Fig. 2B, C). To investigate the role of caspases, neutrophils were treated with the caspase-3/7 inhibitor DEVD-FMK, the caspase-1 inhibitor YVAD-CMK, or the broad-spectrum caspase inhibitor QVD-OPh for 1h prior to treatment with

nigericin. QVD-OPh inhibited nigericin-induced cell death to the same extent as iSK15 after 1h and 4h. The more specific inhibitors DEVD-FMK and YVAD-CMK were less effective at preventing cell death, showing no significant rescue at 1h (Fig. 2B, C). To consolidate the findings, cell death was also quantified by flow cytometry (Fig. 2D, Supplementary Fig. S2C). Upon nigericin treatment, neutrophils became rapidly permeable to SYTOX Green. Pyroptosis was significantly inhibited by iSK15 up to 4h and by caspase inhibitors at 1h (Fig. 2D). Again, broad caspase inhibition by QVD-OPh was more effective than selective caspase inhibition. To test the effects of priming, isolated neutrophils were incubated for 3h with LPS and then treated with nigericin for 1h. LPS priming alone did not induce cell death in neutrophils and nigericin-induced pyroptosis was similarly inhibited by iSK15 pre-treatment (Supplementary Fig. S2C). These data indicate that human neutrophils are susceptible to nigericin-induced pyroptosis mediated by GrA and multiple caspase pathways.

GrA is Not Essential for Mouse Neutrophil Pyroptosis

To complement inhibitor-based studies with a genetic loss-of-function approach, and to determine if the function of GrA in neutrophil pyroptotic cell death is conserved in mice, we evaluated the expression and activity of GrA in bone marrow neutrophils from wild type C57BL/6J (WT) mice and we examined nigericin-induced death in GrA-deficient ($GrA^{-/-}$) murine neutrophils. GrA was barely detectable by western blot and no activity was detected with the SK15.5 ABP in bone marrow mouse neutrophils, whereas GrA protein and activity were detected in human neutrophils and the human natural killer cell line NK92. NE activity was detected in human and mouse neutrophils, but not in NK92 cells (Fig. 3A). To further investigate the presence and function of GrA in mouse granulocytes, bone marrow and blood of WT and $GrA^{-/-}$ mice were analyzed by flow cytometry and isolated neutrophils were stimulated *in vitro* with nigericin. $GrA^{-/-}$ mice had comparable numbers of neutrophils as WT mice in the blood and bone marrow. GrA and perforin expression was confirmed by intracellular staining of blood NK cells from WT mice, while $GrA^{-/-}$ NK cells were negative for GrA and positive for perforin thus validating the specificity of the antibody for mouse GrA. As expected, B cells expressed neither GrA nor perforin. Only a small fraction (2%) of blood and bone marrow neutrophils expressed GrA (Supplementary Fig. S3 A-C). Isolated mouse bone marrow neutrophils from both genotypes were treated with nigericin, which induced significant cell death after 4, 6, and 18h compared to respective untreated controls. However, no significant difference was observed between WT and $GrA^{-/-}$ neutrophils (Fig. 3B). These findings indicate that GrA is expressed in a very small subset of healthy mouse neutrophils and is not an essential mediator of pyroptotic death in these cells.

GrA Contributes to Pyroptosis in Human iPSC-Derived Neutrophils

We then employed iPSC-derived neutrophil-like cells (iPSneu) as an orthogonal human model. Differentiation was confirmed by high surface expression of CD11b and CD16 after 7 days. GrA protein was detected as a punctate cytoplasmic staining by immunofluorescence, consistent with granule

localization (Supplementary Fig. S3G. Nigericin stimulation induced progressive lytic death in iPSneu with dense nuclear staining detectable after 30 min and diffuse cytoplasmic staining from 60 min onwards (Fig. 3C, D). Pre-treatment with iSK15 reduced both membrane disruption and nuclear fragmentation at the early stages of the 4.5h imaging period, while vehicle controls and iSK15 alone had no effect on basal viability (Fig. 3C, D). Thus, GrA inhibition delays nigericin-induced pyroptosis in a donor-independent neutrophil paradigm, based on the iPS cell model, establishing that GrA-dependent pyroptotic execution is a conserved feature of human neutrophil biology. However, given the modest magnitude of the effect and its clearest manifestation at the 1h time point, we considered the model insufficiently robust for further validation and therefore focused subsequent experiments on primary human neutrophils.

GrA Mediates Lysosomal Cell Death but not Neutrophil Spontaneous Apoptosis

We next investigated whether GrA contributes to spontaneous neutrophil apoptosis *in vitro*. Treatment with iSK15 had no effect on the onset of apoptosis and secondary necrosis of primary human neutrophils. As expected, QVD-OPh and DEVD-FMK significantly prevented spontaneous apoptosis through their inhibition of executor caspase-3/7. Surprisingly, YVAD-CMK, a caspase-1 inhibitor, also prevented this form of cell death. This was unexpected, as inhibition of caspase-1, which is primarily associated with pyroptosis rather than apoptosis, would not be expected to block apoptotic cell death (Fig. 4A). Spontaneous death of neutrophils *in vitro* is largely driven by the intrinsic (mitochondrial) pathway of apoptosis and to a lesser extent via the extrinsic (death receptor) pathway. The latter is mediated by caspase-8 and both pathways culminate in the activation of caspase-3 (4). Proteolysis of peptide substrates showed that QVD-OPh, DEVD-FMK, and YVAD-CMK inhibited both caspase-3 and caspase-8, although YVAD was slightly less efficient at inhibiting caspase-3 indicating the relative broad specificities of these inhibitors at the concentrations used. Importantly, iSK15 showed no inhibitory effect on either recombinant purified caspase-3 or caspase-8 (Fig. 4B) (43), establishing that spontaneous neutrophil apoptosis is GrA-independent.

Finally, we tested whether the release of GrA from primary granules into the cytosol contributes to cell death. Neutrophils were stimulated with the lysosomotropic agent LLME, which rapidly induces lysosomal permeabilization and cell death in granule-containing leukocytes (44). iSK15, DEVD-FMK and YVAD-CMK significantly reduced LLME-induced cell death at 2 and 4 h, whereas at 4 h caspase inhibitors DEVD-FMK and YVAD-CMK provided less statistically significant rescue (Fig. 4C). Since LLME induces CatG-dependent cell death in mouse neutrophils (26), cells were pre-treated with a selective CatG inhibitor (iCatG), iSK15, or both prior to LLME stimulation. CatG inhibition alone or combined with iSK15 completely protected neutrophils from LLME-induced death at both time points (Fig. 4D). The specificity of iSK15 toward GrA relative to the other neutrophil serine proteases was confirmed using activity-based probe staining (45). The activity of CatG, NE, and PR3 was not altered by iSK15 (Fig. 4E). Therefore, GrA and CatG act as non-redundant, cooperative drivers of lysosomal membrane permeabilization-induced neutrophil death.

Cytosolic release of granzyme A during pyroptosis

The localisation of GrA during pyroptotic stimulation was assessed by confocal microscopy at early time points following nigericin treatment. In naïve neutrophils, GrA staining displayed the punctate cytoplasmic pattern consistent with primary granule localization, whereas granule permeabilization with LLME expectedly released GrA into the cytosol. Following nigericin stimulation, GrA staining was readily detectable throughout the cytosol after 1h and was no longer confined to discrete granular structures (Fig. 4F). This redistribution was accompanied by the morphological changes characteristic of lytic cell death visible in phase contrast images. Total and active GrA, determined by western blot and ABP, appear to accumulate over 4h in cultured neutrophils, while after 4h of nigericin treatment, total and active GrA levels were significantly decreased (Fig. 4G, H). This reduction of GrA within treated cells was paralleled with the appearance of GrA in neutrophil supernatant suggesting post-lytic release (Fig. 4I). Perforin was not detectable by microscopy in resting or nigericin-stimulated neutrophils (Supplementary Fig. S2D).

GrA cleaves GSDMD and GSDME

GSDMD and GSDME are established mediators of pyroptosis and are both expressed in neutrophils. In addition to caspases, GSDMD and GSDME can be cleaved by neutrophil granule proteases, while GrA has been reported to directly cleave only GSDMB (46–49), which is not expressed in neutrophils. We therefore hypothesised that, upon granule permeabilization, cytosolic GrA contributes to nigericin-induced neutrophil death through the cleavage of GSDMD and/or GSDME. As GrA is an Arg-specific protease, it cannot cleave at the canonical aspartate residues recognized by the inflammatory and apoptotic caspases (GSDMD Asp275; GSDME Asp270) (50–52). Lysates of cells overexpressing GSDMD, GSDME, GSDMB, or NINJ1 were incubated with GrA, with untreated lysate as a time-matched control. GrA cleaved GSDMD within 1 h, producing three distinct fragments of approximately 46, 26, and 15 kDa (Fig. 5A; Full-length uncropped original western blots are provided in Supplementary File 1). To map likely GrA cleavage sites within GSDMD, we designed a panel of internally quenched fluorogenic (IQF) octapeptide substrates encompassing candidate Arg cleavage sites inferred from the fragments sizes. In each substrate, the putative P1 residue was Arg and was flanked by residues occupying positions P6–P2 and P1'–P2 (Supplementary Fig. S4). The substrate library was screened with purified GrA enabling the determination of the hydrolysis rate (RFU/s) for each peptide. The substrates exhibiting the highest hydrolysis rates were considered to represent the most likely GrA cleavage sites within the full-length proteins. Based on these analyses, GrA most likely cleaves GSDMD after Arg465, Arg267 and Arg151 (Fig. 5B), which match the fragment sizes of 46, 26 and 15 kDa observed by western blot (Fig. 5A). In a similar analysis, GrA also cleaved GSDME to generate a fragment of approximately 25 kDa, detected with an N-terminal-specific antibody (Fig. 5C). The putative cleavage site was investigated using a similarly designed IQF peptide library focused on Arg residues of GSDME and Arg119 appears the most likely residue for GSDME cleavage of GrA (Fig. 5D). To rule out indirect activation of caspases by GrA and subsequent processing of GSDMD and GSDME, lysates were pre-incubated with the pan-caspase inhibitor QVD-OPh prior to GrA addition. Caspase inhibition did not affect GrA-mediated cleavage of

gasdermins indicating direct proteolytic processing by GrA (Fig. 5E, 5F). GrA also cleaved GSDMB to generate two products of approximately 30 kDa and 17 kDa, corresponding to the previously described activating cleavage within the interdomain linker (Fig. 5G). NINJ1, which mediates plasma membrane rupture after gasdermin activation, was not cleaved by GrA at any timepoint, serving as a negative control (Fig. 5H). To compare GrA-mediated cleavage with other immune cell granule proteases, lysates were incubated with a panel of granzymes and NSPs (1 h for granzymes and 15 min for other NSPs). GSDMD was cleaved by GrK, GrM, GrB, CatG, and NSP4, while NE and PR3 appear to rapidly degrade GSDMD (Fig. 5I). In contrast, GSDME was cleaved by GrA, GrK, GrB, NE, CatG, and PR3 (Fig. 5J). Notably, each protease generated a distinct cleavage pattern, consistent with proteolysis at different cleavage sites. Overall, our data suggests that GrA principally disarms GSDMD and GSDME via proteolysis in their N-terminal domains at R151/R153 and R119, respectively. However, the R267 cleavage site of the interdomain linker may activate GSDMD through a non-canonical processing (Fig. 5K).

GrA spatially converges with GSDME during pyroptosis and drives ROS generation upstream of membrane rupture

We next investigated whether gasdermins spatially associate with GrA during nigericin-induced death. Freshly isolated neutrophils pre-treated or not with iSK15 for 1h were stimulated with nigericin for 0, 0.5, or 1h and analyzed by immunofluorescence confocal microscopy (Fig. 6A). Nigericin stimulation increased colocalization of GSDMD with GrA over time ($r \sim 0.4$ to ~ 0.6, $p < 0.0001$) (Fig. 6C). Neutrophils pre-treated with iSK15 showed a higher baseline co-localization of GrA and GSDMD but treatment with nigericin induced a significant reduction of GSDMD colocalization with GrA after 1h ($p < 0.0001$) (Fig. 6C). Similarly, GSDME colocalization with GrA increased during nigericin stimulation ($r \sim 0.4$ to ~ 0.6, $p < 0.0001$) (Fig. 6B). In neutrophils pre-treated with iSK15, pre-treatment further increased GrA colocalization with GSDME on average ($p < 0.0001$) (Fig. 6D). Interestingly, we observed the emergence of two distinct cell populations after 1h of nigericin treatment in presence of iSK15: one population was comparable to pyroptotic cells treated with nigericin alone, showing high GrA-GSDME colocalization (r approximately 0.5), whereas the second population exhibited a markedly lower r (approximately 0.2) and neutrophils appeared as unstimulated healthy cells (Fig. 6B, D).

Because GrA is known to perturb mitochondrial function and promote ROS generation in cytotoxic lymphocyte contexts (53), we asked whether GrA contributes to the ROS observed during neutrophil pyroptosis. ROS production was monitored by CellROX live-cell imaging and flow cytometry following nigericin stimulation. Nigericin induced a rapid and progressive increase in ROS (Fig. 6E, G), reaching almost 40% of CellROX positivity within 30 min in live imaging. Pre-treatment with iSK15 delayed and reduced ROS accumulation (Fig. 6E, G). Flow cytometry analysis confirmed these findings with iSK15 significantly reducing the proportion of CellROX-positive cells at 10, 20, and 30 min post-induction (Fig. 6F). Together, these data demonstrate that GrA promotes inflammasome-induced ROS generation and modifies the cellular localization of GSDMD and GSDME.

Discussion

Neutrophil death is regulated by an unusually protease-rich intracellular environment in which disruption of granule integrity can rapidly expose cytosolic substrates to enzymes that are normally sequestered within granules. Granule serine proteases have previously been implicated in the regulation and execution of several neutrophil cell death pathways (54), however the presence and biological role of granzyme A (GrA) in neutrophils was previously obscure and somewhat controversial (28, 29, 55, 56).

Establishing this function first required resolving the longstanding uncertainty over whether GrA is present in human neutrophils. Previous studies reached conflicting conclusions: some reported that human neutrophils lack GrA, GrB and perforin, whereas others provided evidence of GrA expression in polymorphonuclear neutrophils (28, 56, 57). In studies in which GrA was detected, it was proposed to localize predominantly to peroxidase-negative rather than primary azurophilic granules (28). In contrast, our data place the predominant GrA pool in primary granules, together with the neutrophil serine proteases NE, PR3, CatG and NSP4 (Fig. 1B, C). This localization provides a framework in which sequestration within primary granules restricts GrA access to intracellular substrates. Thus, GrA function may be determined not only by its expression, but also by its compartmentalization. Demonstrating that granule-associated GrA is catalytically active is therefore particularly important, as it establishes its capacity to participate in proteolytic events following loss of granule integrity (Fig. 1D, E).

Selective pharmacological inhibition of GrA delayed and reduced LLME-induced death resulting from granule permeabilization in primary human neutrophils (Fig. 4C, D). A similar protective effect was observed following nigericin-induction, whereas GrA inhibition did not affect spontaneous neutrophil apoptosis (Fig. 4A). These findings indicate that GrA contributes specifically to lytic neutrophil death. However, because inhibition delayed rather than completely prevented membrane permeabilization, GrA appears to regulate the rate and efficiency of death rather than act as an indispensable executioner (Fig. 2B-D). This distinction is particularly relevant in neutrophils, where multiple granule proteases can be released into the same intracellular compartment and may act on substrates from overlapping or parallel pathways (58, 59). The LLME treatment therefore provides a useful framework for placing GrA within this broader proteolytic network (44, 60).

The nigericin activation extends the role of GrA beyond direct pharmacological permeabilization of neutrophil granules. Nigericin is widely used to activate the NLRP3 (NOD-, LRR- and pyrin domain-containing protein 3) inflammasome by disrupting intracellular potassium homeostasis, but its effects depend strongly on concentration, cell type and experimental context (61–63). In macrophage-like cells, low concentrations predominantly induce caspase-1- and GSDMD-dependent death, whereas higher concentrations can cause rapid lysis that becomes resistant to inhibition of canonical inflammasome-associated proteases (64–66). At intermediate concentrations, lysosomal protease inhibition can delay membrane damage, suggesting that lysosomal leakage may amplify rather than initiate the death response (67–69). With stronger ionic disturbance, this regulatory contribution can be bypassed by irreversible organellar and membrane damage.

These findings from macrophage models cannot be directly extrapolated to primary human neutrophils, and 10 μM nigericin should not be assumed to have the same mechanistic consequences across cell types. Nevertheless, they provide a useful framework for interpreting the incomplete protection observed after GrA inhibition (Fig. 2C, D). Nigericin may initiate cell death independently of GrA, while concomitant granule destabilization releases GrA and other azurophilic proteases that accelerate downstream membrane damage (Fig. 4F). In this model, GrA inhibition reduces the efficiency of death execution without reversing the initial commitment to die, leaving sufficient parallel proteolytic and membrane-damaging activity to permit eventual cell death. Consistent with a function following loss of granule compartmentalization, GrA redistributed from a punctate granular pattern into the cytosol after both LLME and nigericin stimulation (Fig. 4F). During nigericin-induced death, GrA remained predominantly intracellular at early stages and became detectable extracellularly at later time points, coincident with extensive loss of plasma membrane integrity (Fig. 2B, C). These observations favor an intracellular function for GrA during the execution phase of neutrophil death rather than a mechanism driven primarily by extracellular GrA. We therefore propose that granule permeabilization exposes GrA to cytosolic substrates that are normally physically separated from the enzyme.

Gasdermins represent attractive candidate substrates for GrA because their biological function is determined by proteolytic processing in pyroptosis (46, 49). In neutrophils, GSDMD activity is strongly influenced by intracellular localization. Karmakar et al. showed that N-terminal GSDMD generated during inflammasome activation can associate with intracellular organelles, including azurophilic granules, rather than exclusively forming plasma-membrane pores (70). Therefore, even a GrA-generated GSDMD fragment with potential pore-forming activity would not necessarily result in canonical pyroptosis. This interpretation is further supported by Tschopp et al., who showed that GrA can process pro-IL-1β without generating the mature, bioactive cytokine, indicating that GrA-mediated proteolysis does not necessarily lead to activation of substrates associated with pyroptotic signaling (71). A minor pool of activation-competent GSDMD could instead act at intracellular membranes and contribute to granule permeabilization and protease redistribution. In addition, GrA has previously been linked to caspase-independent perturbation of mitochondrial function and generation of ROS in target cells exposed to cytotoxic lymphocytes (53). Consistent with a possible role in oxidative stress, GrA inhibition reduced intracellular ROS generation following nigericin stimulation in our experiments (Fig. 6E, F). Whether this reflects direct GrA-dependent mitochondrial damage, an indirect consequence of delayed lytic progression, or another proteolytic pathway remains unresolved. Nevertheless, these findings suggest that GrA may promote neutrophil death through mechanisms that extend beyond gasdermin activation.

GrA-mediated processing of GSDMD and GSDME is more likely consistent with their inactivation (Fig. 5A, C). Thus, our results suggest that GrA promotes early death through additional intracellular substrates, while gasdermin processing represents a parallel or later regulatory event. Alternatively, the biological activity of the individual GrA-generated gasdermin fragments may differ from that predicted solely from their cleavage position. Direct functional characterization of these fragments will therefore be required to determine their contribution to neutrophil death.

Such heterogeneous processing is not unprecedented in neutrophils. CatG can generate an activating GSDMD fragment near the inflammatory caspase cleavage site, whereas other granule proteases produce distinct fragments or promote more extensive GSDMD degradation (25). Consistent with this, we observed protease-specific fragmentation of GSDMD and GSDME by different neutrophil serine proteases and granzymes (Fig. 5I, J). These findings suggest that gasdermins in neutrophils are shaped by competing proteolytic events rather than acting as simple binary switches. The distinct effects of CatG and GrA inhibition further indicate non-equivalent roles in cell death, with CatG providing a stronger death-driving activity and GrA modifying the kinetics or trajectory of the response. Whether they act on separate substrates, converge on common targets at different sites, or participate in sequential proteolytic events remains to be determined.

Our study identifies GrA as a cell-intrinsic component of a granule-linked neutrophil death pathway. GrA was predominantly associated with primary granules, and pharmacological inhibition of GrA protected neutrophils from death induced by either LLME or nigericin. The magnitude of protection was not altered by LPS priming. GrA remained cell associated during the early phase of nigericin-induced death and became extracellular only later, whereas GrA inhibition reduced the ROS response. Together, these findings support a model in which intracellular stress makes preformed GrA functionally available inside neutrophils, coupling granule perturbation to oxidative and proteolytic events that promote death. This function extends the earlier demonstration that human neutrophils constitutively express GrA (28).

Declarations

Conflict of interest

The authors declare that the research was conducted in the absence of any commercial or financial relationships that could be construed as a potential conflict of interest.

Availability of Data and Materials

The analyzed data supporting the findings of this study are provided within the article and its Supporting Information. Raw flow cytometry, confocal microscopy, and kinetic data are available from the corresponding author upon reasonable request. No custom code or software was generated as part of this study.

Author contributions

AKM, CB and PK conceived and designed the study. AKM designed and performed experiments, acquired data, analysed and interpreted results, prepared figures, wrote the manuscript. EB performed experiments, acquired and analysed results. RP, JM - Synthesized and purified GSDMD and GSDME substrates. KS performed the chemical synthesis of the compounds, performed experiments. KDK design of constructs for transfection, performed experiments. NK and MB contributed to experiments with mouse neutrophils, analysed results. GS contributed reagents and writing and revising the

manuscript. SS, JWT, and DK contributed enzymes. SP contributed blood samples. SK developed SK15i and SK15.5. CB, PK biological analyses and data interpretation, writing and editing the manuscript, figure preparation, revision and discussion funding acquisition. All authors discussed the results, contributed to the final version of the manuscript, and approved it for publication.

Acknowledgements:

The author(s) declare that financial support was received for the research and/or publication of this article. This project was financed by a grant from the National Science Centre; OPUS 2020/39/B/NZ1/03027 awarded to PK, and in part by a grant from the Swiss National Science Foundation (SNSF 212380) to CB.

References

1. Tak T, Tesselaar K, Pillay J, Borghans JAM, Koenderman L. What's your age again? Determination of human neutrophil half-lives revisited. Journal of Leukocyte Biology. 2013;94(4):595–601.
2. Kruger P, Saffarzadeh M, Weber AN, Rieber N, Radsak M, von Bernuth H, et al. Neutrophils: Between host defence, immune modulation, and tissue injury. PLoS Pathog. 2015;11(3):e1004651.
3. Ballesteros I, Hidalgo A. The neutrophil collective. Cell. 2025;188(25):7019–35.
4. Geering B, Simon HU. Peculiarities of cell death mechanisms in neutrophils. Cell Death & Differentiation. 2011;18(9):1457–69.
5. Zhang J, Shao Y, Wu J, Zhang J, Xiong X, Mao J, et al. Dysregulation of neutrophil in sepsis: recent insights and advances. Cell Communication and Signaling. 2025;23(1):87.
6. Lakshman R, Finn A. Neutrophil disorders and their management. J Clin Pathol. 2001;54(1):7–19.
7. Fu X, Liu H, Huang G, Dai SS. The emerging role of neutrophils in autoimmune-associated disorders: effector, predictor, and therapeutic targets. MedComm (2020). 2021;2(3):402 – 13.
8. De Filippo K, Rankin SM. CXCR4, the master regulator of neutrophil trafficking in homeostasis and disease. Eur J Clin Invest. 2018;48 Suppl 2(Suppl Suppl 2):e12949.
9. Hidalgo A, Chilvers ER, Summers C, Koenderman L. The Neutrophil Life Cycle. Trends Immunol. 2019;40(7):584–97.
10. Stark MA, Huo Y, Burcin TL, Morris MA, Olson TS, Ley K. Phagocytosis of apoptotic neutrophils regulates granulopoiesis via IL-23 and IL-17. Immunity. 2005;22(3):285–94.
11. Casanova-Acebes M, Pitaval C, Weiss LA, Nombela-Arrieta C, Chevre R, N AG, et al. Rhythmic modulation of the hematopoietic niche through neutrophil clearance. Cell. 2013;153(5):1025–35.
12. Rogers C, Fernandes-Alnemri T, Mayes L, Alnemri D, Cingolani G, Alnemri ES. Cleavage of DFNA5 by caspase-3 during apoptosis mediates progression to secondary necrotic/pyroptotic cell death. Nat Commun. 2017;8:14128.
13. Rogers C, Erkes DA, Nardone A, Aplin AE, Fernandes-Alnemri T, Alnemri ES. Gasdermin pores permeabilize mitochondria to augment caspase-3 activation during apoptosis and inflammasome

activation. Nature Communications. 2019;10(1):1689.

14. Brinkmann V, Reichard U, Goosmann C, Fauler B, Uhlemann Y, Weiss DS, et al. Neutrophil extracellular traps kill bacteria. Science. 2004;303(5663):1532–5.
15. Sollberger G, Amulic B, Zychlinsky A. Neutrophil Extracellular Trap Formation Is Independent of De Novo Gene Expression. PLoS One. 2016;11(6):e0157454.
16. Boeltz S, Amini P, Anders HJ, Andrade F, Bilyy R, Chatfield S, et al. To NET or not to NET:current opinions and state of the science regarding the formation of neutrophil extracellular traps. Cell Death Differ. 2019;26(3):395–408.
17. Yousefi S, Stojkov D, Germic N, Simon D, Wang X, Benarafa C, et al. Untangling "NETosis" from NETs. Eur J Immunol. 2019;49(2):221–7.
18. Pérez-Figueroa E, Álvarez-Carrasco P, Ortega E, Maldonado-Bernal C. Neutrophils: Many Ways to Die. Frontiers in Immunology. 2021;Volume 12–2021.
19. Pham CT. Neutrophil serine proteases: specific regulators of inflammation. Nat Rev Immunol. 2006;6(7):541–50.
20. Sullivan GP, Davidovich P, Munoz-Wolf N, Ward RW, Hernandez Santana YE, Clancy DM, et al. Myeloid cell-derived proteases produce a proinflammatory form of IL-37 that signals via IL-36 receptor engagement. Sci Immunol. 2022;7(78):eade5728.
21. Leborgne NG, Devisme C, Kozarac N, Berenguer Veiga I, Ebert N, Godel A, et al. Neutrophil proteases are protective against SARS-CoV-2 by degrading the spike protein and dampening virus-mediated inflammation. JCI Insight. 2024;9(7).
22. Shagirova A, Allayarova M, Makhanova A, Bekturgan A, Burster T. A Double-Edged Sword: Extracellular Serine Proteases as Facilitators of Infection and Mediators of Immunity. Molecules. 2026;31(4).
23. Arreba-Tutusaus P, Borbaran-Bravo N, Doll L, Ritter M, Kretschmer D, Haaf J, et al. Inherited disorders of granulopoiesis: understanding pathogenesis to advance new therapies. Exp Hematol. 2026;158:105418.
24. Benarafa C, LeCuyer TE, Baumann M, Stolley JM, Cremona TP, Remold-O'Donnell E. SerpinB1 protects the mature neutrophil reserve in the bone marrow. J Leukoc Biol. 2011;90(1):21–9.
25. Burgener SS, Leborgne NGF, Snipas SJ, Salvesen GS, Bird PI, Benarafa C. Cathepsin G Inhibition by Serpinb1 and Serpinb6 Prevents Programmed Necrosis in Neutrophils and Monocytes and Reduces GSDMD-Driven Inflammation. Cell Rep. 2019;27(12):3646-56.e5.
26. Baumann M, Pham CT, Benarafa C. SerpinB1 is critical for neutrophil survival through cell-autonomous inhibition of cathepsin G. Blood. 2013;121(19):3900-7, S1-6.
27. Smyth MJ, O'Connor MD, Trapani JA. Granzymes: a variety of serine protease specificities encoded by genetically distinct subfamilies. J Leukoc Biol. 1996;60(5):555–62.
28. Hochegger K, Eller P, Huber JM, Bernhard D, Mayer G, Zlabinger GJ, et al. Expression of granzyme A in human polymorphonuclear neutrophils. Immunology. 2007;121(2):166–73.

29. Metkar SS, Froelich CJ. Human neutrophils lack granzyme A, granzyme B, and perforin. Blood. 2004;104(3):905–6.
30. Martinvalet D, Zhu P, Lieberman J. Granzyme A induces caspase-independent mitochondrial damage, a required first step for apoptosis. Immunity. 2005;22(3):355–70.
31. Chowdhury D, Lieberman J. Death by a thousand cuts: granzyme pathways of programmed cell death. Annu Rev Immunol. 2008;26:389–420.
32. Kolt S, Janiszewski T, Kaiserman D, Modrzycka S, Snipas SJ, Salvesen G, et al. Detection of Active Granzyme A in NK92 Cells with Fluorescent Activity-Based Probe. J Med Chem. 2020;63(6):3359–69.
33. Trump LR, Nayak RC, Singh AK, Emberesh S, Wellendorf AM, Lutzko CM, et al. Neutrophils Derived from Genetically Modified Human Induced Pluripotent Stem Cells Circulate and Phagocytose Bacteria In Vivo. Stem Cells Transl Med. 2019;8(6):557–67.
34. Lachmann N, Ackermann M, Frenzel E, Liebhaber S, Brennig S, Happle C, et al. Large-scale hematopoietic differentiation of human induced pluripotent stem cells provides granulocytes or macrophages for cell replacement therapies. Stem Cell Reports. 2015;4(2):282–96.
35. Cruvinel E, Ogusuku I, Cerioni R, Rodrigues S, Gonçalves J, Góes ME, et al. Long-term single-cell passaging of human iPSC fully supports pluripotency and high-efficient trilineage differentiation capacity. SAGE Open Med. 2020;8:2050312120966456.
36. Çelik E, Çalık P, Oliver SG. Fed-batch methanol feeding strategy for recombinant protein production by Pichia pastoris in the presence of co-substrate sorbitol. Yeast. 2009;26(9):473–84.
37. Bovenschen N, Quadir R, van den Berg AL, Brenkman AB, Vandenberghe I, Devreese B, et al. Granzyme K Displays Highly Restricted Substrate Specificity That Only Partially Overlaps with Granzyme A*. Journal of Biological Chemistry. 2009;284(6):3504–12.
38. Tang W, Ultsch M, Adaligil E, Tombling B, Fleming S, Wei Y, et al. Novel Macrocyclic Peptides as Potent and Selective Inhibitors of Human Neutrophil Serine Protease 4. J Mol Biol. 2026;438(19):169894.
39. Poreba M, Szalek A, Rut W, Kasperkiewicz P, Rutkowska-Wlodarczyk I, Snipas SJ, et al. Highly sensitive and adaptable fluorescence-quenched pair discloses the substrate specificity profiles in diverse protease families. Sci Rep. 2017;7:43135.
40. Maly DJ, Leonetti F, Backes BJ, Dauber DS, Harris JL, Craik CS, et al. Expedient Solid-Phase Synthesis of Fluorogenic Protease Substrates Using the 7-Amino-4-carbamoylmethylcoumarin (ACC) Fluorophore. The Journal of Organic Chemistry. 2002;67(3):910–5.
41. Kjeldsen L, Bainton DF, Sengeløv H, Borregaard N. Structural and functional heterogeneity among peroxidase-negative granules in human neutrophils: identification of a distinct gelatinase-containing granule subset by combined immunocytochemistry and subcellular fractionation. Blood. 1993;82(10):3183–91.
42. Faurschou M, Borregaard N. Neutrophil granules and secretory vesicles in inflammation. Microbes and Infection. 2003;5(14):1317–27.

43. Pereira NA, Song Z. Some commonly used caspase substrates and inhibitors lack the specificity required to monitor individual caspase activity. Biochemical and Biophysical Research Communications. 2008;377(3):873–7.
44. Thiele DL, Lipsky PE. Mechanism of L-leucyl-L-leucine methyl ester-mediated killing of cytotoxic lymphocytes: dependence on a lysosomal thiol protease, dipeptidyl peptidase I, that is enriched in these cells. Proc Natl Acad Sci U S A. 1990;87(1):83–7.
45. Kasperkiewicz P, Altman Y, D'Angelo M, Salvesen GS, Drag M. Toolbox of Fluorescent Probes for Parallel Imaging Reveals Uneven Location of Serine Proteases in Neutrophils. Journal of the American Chemical Society. 2017;139(29):10115–25.
46. Zhou Z, He H, Wang K, Shi X, Wang Y, Su Y, et al. Granzyme A from cytotoxic lymphocytes cleaves GSDMB to trigger pyroptosis in target cells. Science. 2020;368(6494).
47. Oltra SS, Colomo S, Sin L, Pérez-López M, Lázaro S, Molina-Crespo A, et al. Distinct GSDMB protein isoforms and protease cleavage processes differentially control pyroptotic cell death and mitochondrial damage in cancer cells. Cell Death Differ. 2023;30(5):1366–81.
48. Zhong X, Zeng H, Zhou Z, Su Y, Cheng H, Hou Y, et al. Structural mechanisms for regulation of GSDMB pore-forming activity. Nature. 2023;616(7957):598–605.
49. Zhong X, Su Y, Zhou Z, Sun Y, Hou Y, Shao F, et al. Exosite-mediated targeting of GSDMB by dimeric granzyme A in lymphocyte pyroptotic killing. Immunity. 2026;59(2):257 – 69.e6.
50. Aglietti RA, Estevez A, Gupta A, Ramirez MG, Liu PS, Kayagaki N, et al. GsdmD p30 elicited by caspase-11 during pyroptosis forms pores in membranes. Proceedings of the National Academy of Sciences. 2016;113(28):7858-63.
51. Taabazuing CY, Okondo MC, Bachovchin DA. Pyroptosis and Apoptosis Pathways Engage in Bidirectional Crosstalk in Monocytes and Macrophages. Cell Chem Biol. 2017;24(4):507 – 14.e4.
52. Wang Y, Gao W, Shi X, Ding J, Liu W, He H, et al. Chemotherapy drugs induce pyroptosis through caspase-3 cleavage of a gasdermin. Nature. 2017;547(7661):99–103.
53. Martinvalet D, Dykxhoorn DM, Ferrini R, Lieberman J. Granzyme A cleaves a mitochondrial complex I protein to initiate caspase-independent cell death. Cell. 2008;133(4):681–92.
54. Benarafa C, Simon HU. Role of granule proteases in the life and death of neutrophils. Biochem Biophys Res Commun. 2017;482(3):473–81.
55. Hochegger K, Eller P, Rosenkranz AR. Granzyme A: an additional weapon of human polymorphonuclear neutrophils (PMNs) in innate immunity? Blood. 2004;103(3):1176.
56. Grossman WJ, Ley TJ. Granzymes A and B are not expressed in human neutrophils. Blood. 2004;104(3):906–7; author reply 7–8.
57. Wagner C, Iking-Konert C, Denefleh B, Stegmaier S, Hug F, Hänsch GM. Granzyme B and perforin: constitutive expression in human polymorphonuclear neutrophils. Blood. 2004;103(3):1099–104.
58. Pham CT. Neutrophil serine proteases fine-tune the inflammatory response. Int J Biochem Cell Biol. 2008;40(6–7):1317–33.

59. Miller BA, Horan K, Abbott DW, Pearlman E, Dubyak GR. Perturbation of azurophilic granule integrity drives NLRP3-independent IL-1β processing and release in neutrophils. The Journal of Immunology. 2026;215(3):vkag033.
60. Thiele DL, Lipsky PE. The immunosuppressive activity of L-leucyl-L-leucine methyl ester: selective ablation of cytotoxic lymphocytes and monocytes. The Journal of Immunology. 1986;136(3):1038–48.
61. Cao J, Li L, Yao Y, Xing Y, Ma H. Dehydroepiandrosterone exacerbates nigericin-induced abnormal autophagy and pyroptosis via GPER activation in LPS-primed macrophages. Cell Death & Disease. 2022;13(4):372.
62. Rozario P, Pinilla M, Gorse L, Vind AC, Robinson KS, Toh GA, et al. Mechanistic basis for potassium efflux–driven activation of the human NLRP1 inflammasome. Proceedings of the National Academy of Sciences. 2024;121(2):e2309579121.
63. den Hartigh AB, Fink SL. Pyroptosis Induction and Detection. Curr Protoc Immunol. 2018;122(1):e52.
64. Russo HM, Rathkey J, Boyd-Tressler A, Katsnelson MA, Abbott DW, Dubyak GR. Active Caspase-1 Induces Plasma Membrane Pores That Precede Pyroptotic Lysis and Are Blocked by Lanthanides. J Immunol. 2016;197(4):1353–67.
65. Kayagaki N, Warming S, Lamkanfi M, Walle LV, Louie S, Dong J, et al. Non-canonical inflammasome activation targets caspase-11. Nature. 2011;479(7371):117–21.
66. Mouasni S, Gonzalez V, Schmitt A, Bennana E, Guillonneau F, Mistou S, et al. The classical NLRP3 inflammasome controls FADD unconventional secretion through microvesicle shedding. Cell Death & Disease. 2019;10(3):190.
67. Alu A, Han X, Ma X, Wu M, Wei Y, Wei X. The role of lysosome in regulated necrosis. Acta Pharmaceutica Sinica B. 2020;10(10):1880–903.
68. Repnik U, Hafner Česen M, Turk B. Lysosomal membrane permeabilization in cell death: Concepts and challenges. Mitochondrion. 2014;19:49–57.
69. Brojatsch J, Lima H, Jr., Palliser D, Jacobson LS, Muehlbauer SM, Furtado R, et al. Distinct cathepsins control necrotic cell death mediated by pyroptosis inducers and lysosome-destabilizing agents. Cell Cycle. 2015;14(7):964–72.
70. Karmakar M, Minns M, Greenberg EN, Diaz-Aponte J, Pestonjamasp K, Johnson JL, et al. N-GSDMD trafficking to neutrophil organelles facilitates IL-1β release independently of plasma membrane pores and pyroptosis. Nat Commun. 2020;11(1):2212.
71. Martinon F, Burns K, Tschopp J. The inflammasome: a molecular platform triggering activation of inflammatory caspases and processing of proIL-beta. Mol Cell. 2002;10(2):417–26.

Tables

Table 1 is available in the Supplementary Files section.

Figures

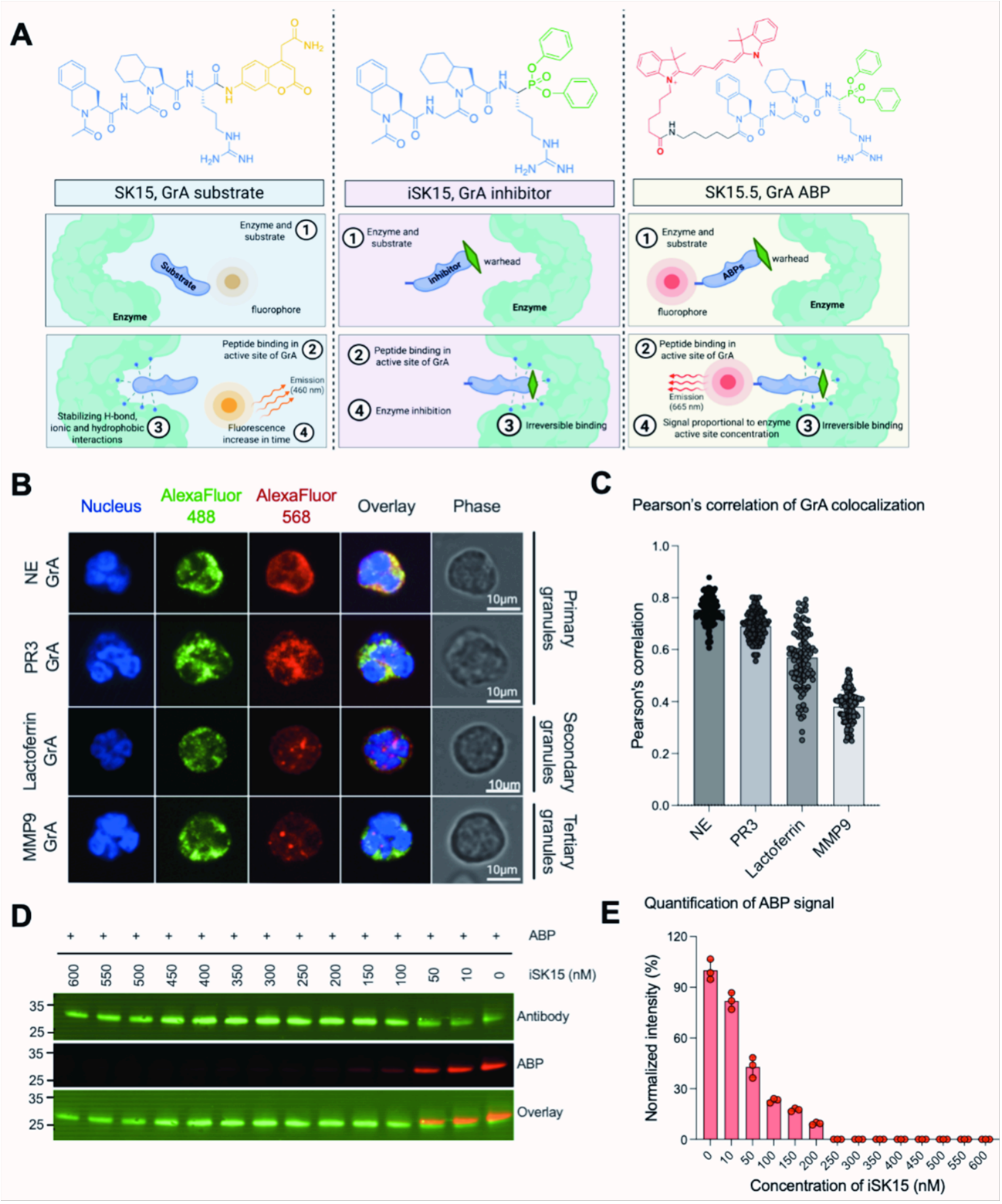


Figure 1

Granzyme A is stored in active form in primary granules of human neutrophils.
(A) Chemical structures and mechanism of action of the GrA-selective fluorogenic substrate SK15, covalent inhibitor iSK15, and activity-based probe (ABP) SK15.5. **(B)**Representative confocal microscopy

images of freshly isolated human neutrophils co-stained with antibodies against GrA (AlexaFluor 568, red) and markers of primary granules (neutrophil elastase, NE; proteinase 3, PR3), secondary granules (lactoferrin), or tertiary granules (MMP9) (AlexaFluor 488, green). Nuclei were counterstained with Hoechst (blue). Scale bars, 10 µm. **(C)**Pearson's correlation coefficients quantifying colocalization of GrA with each granule marker. Each data point represents one cell; n > 100 cells per condition. Bars represent mean ± SD. **(D)** Western blot analysis of GrA activity in freshly isolated neutrophil lysates pre-incubated with increasing concentrations of iSK15 (0–600 nM) prior to labelling with SK15.5 ABP. GrA was detected by anti-GrA antibody (AlexaFluor 488, green) and ABP (Cy5, red). Overlay shown in bottom panel. **(E)** Quantification of ABP signal intensity relative to the concentration of iSK15 used to titrate the ABP.

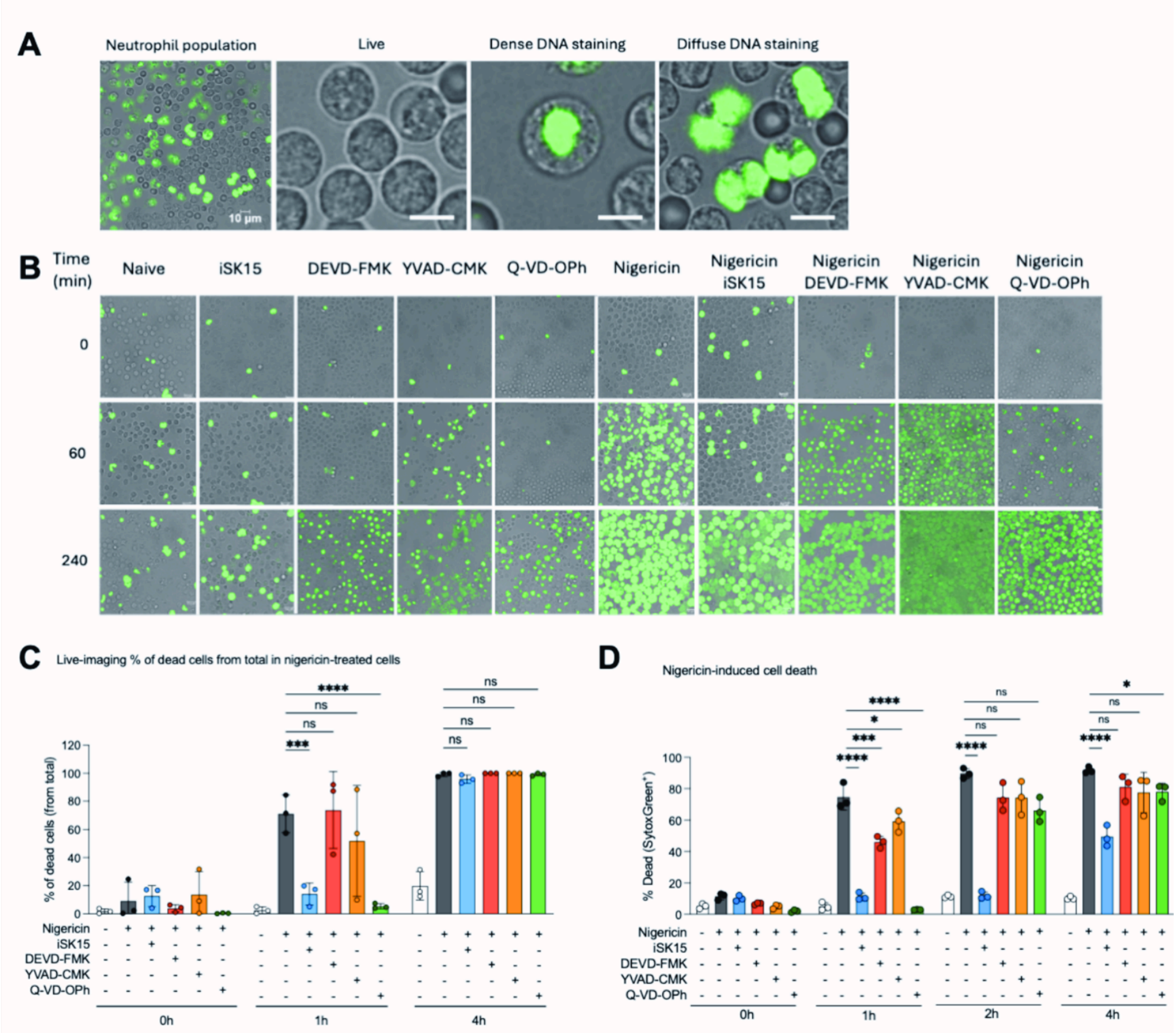


Figure 2

GrA inhibition delays nigericin-induced neutrophil death more effectively than caspase inhibition.

(A) Representative confocal images for classification of cell death stages. The images represent; live cells, dead cells with dense nuclear staining or diffuse DNA staining. Cells stained with SYTOX Green, scale bars 10 μm. **(B)** Representative confocal live-cell images of freshly isolated human neutrophils pre-treated for 1 h with iSK15, DEVD-FMK, YVAD-CMK, or QVD-OPh prior to stimulation with nigericin. SYTOX Green was added at the start of imaging to label cells with compromised plasma membrane integrity. Images were acquired every 30 min over 4 h using a Leica DMi8 inverted confocal microscope (63× oil immersion objective, ex. 488nm). Representative images at 0, 1, and 4h are shown. Scale bars 10 μm. **(C)**Quantification of dead cells 0, 1 and 4h post-nigericin addition by live-imaging microscopy. Data represent mean values from n = 3 independent experiments, each performed on neutrophils isolated from a different healthy donor. **(D)** Flow cytometry analysis of nigericin-induced cell death. Neutrophils pre-treated for 1 h with iSK15, DEVD-FMK, YVAD-CMK, or QVD-OPh were stimulated with nigericin and assessed by flow cytometry as the percentage of SYTOX Green-positive cells at the indicated time points. Bars represent mean ± SD; individual data points represent n = 3 independent experiments each performed on neutrophils from a different healthy donor.

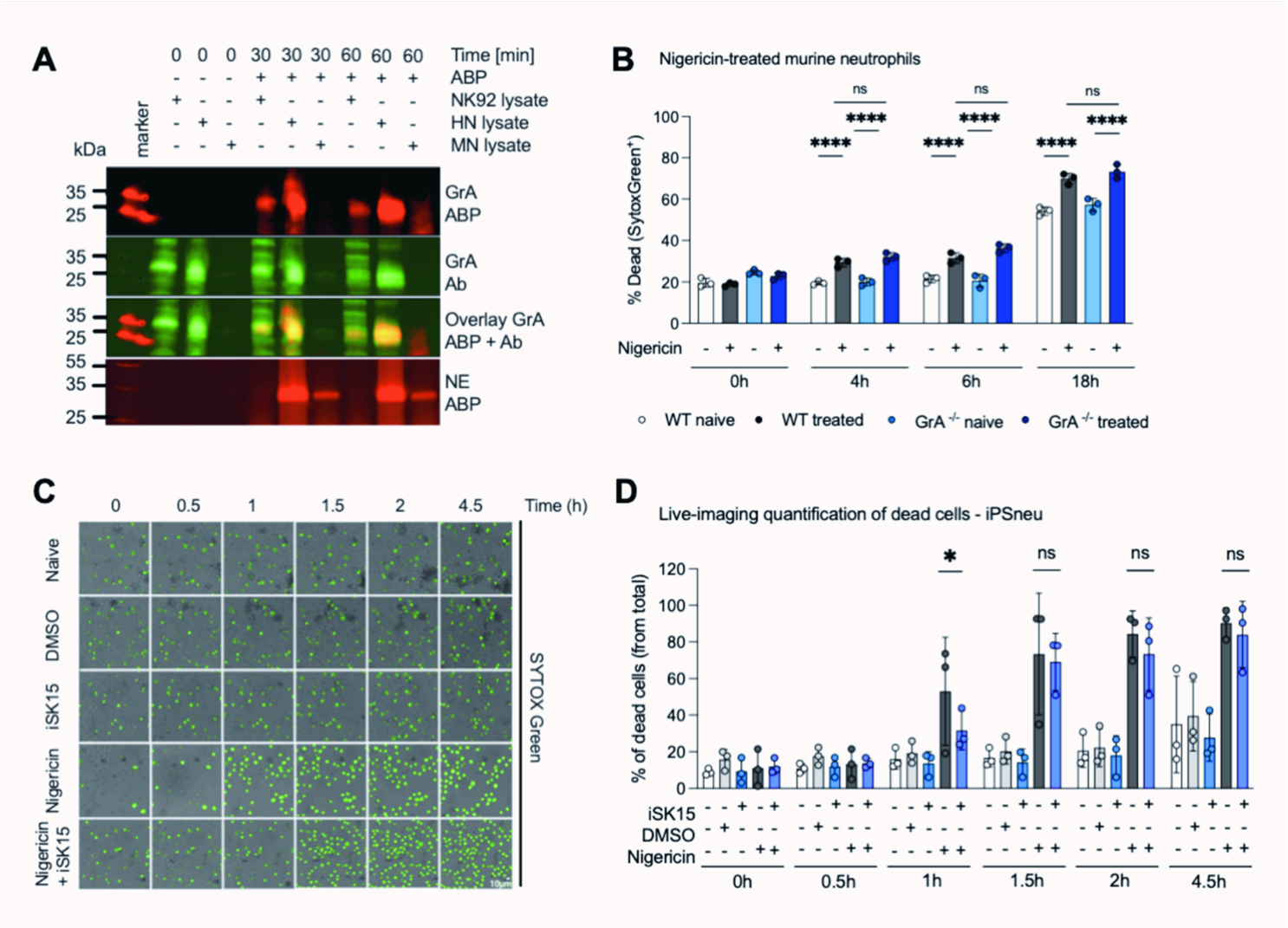


Figure 3

GrA-dependent pyroptosis in human iPSC-derived neutrophils but not in murine neutrophils (A) Western blot analysis of GrA activity and protein in NK92 cell lysates, human neutrophil (HN) lysates, and murine neutrophil (MN) lysates at 0, 30, and 60 min following ABP labelling with SK15.5 (GrA ABP, Cy5, red) and anti-GrA antibody (AlexaFluor 488, green). NE ABP was included as a positive control for protease activity in murine cells. **(B)**Cell death in nigericin-stimulated bone marrow neutrophils from WT and $GrA^{-/-}$ mice assessed by 7-AAD flow cytometry at 0, 4, 6, and 18 h. Data represent mean ± SD; n = 3 independent experiments from different mice. **(C)** Representative confocal live-cell images of iPSneu pre-treated ± 500 nM iSK15 and stimulated with 10 μM nigericin. SYTOX Green (1 μM) was used to label cells with compromised membrane integrity. Images acquired at 0, 30, 60, 90, 120, and 270 min. The images represent; live cells, dead cells with dense nuclear staining or diffuse DNA staining. Scale bar, 10 μm. **(D)** Quantification of dead cells during live imaging in (C). Data represent mean values from n = 3 independent differentiation preparations. Data represent mean ± SD; n = 3 independent batches of iPSneu cells. Statistical comparisons by two-way ANOVA with Šídák's multiple comparisons test; ns, not significant; *$p < 0.05$; **$p < 0.01$;***p < 0.001; ****p < 0.0001.

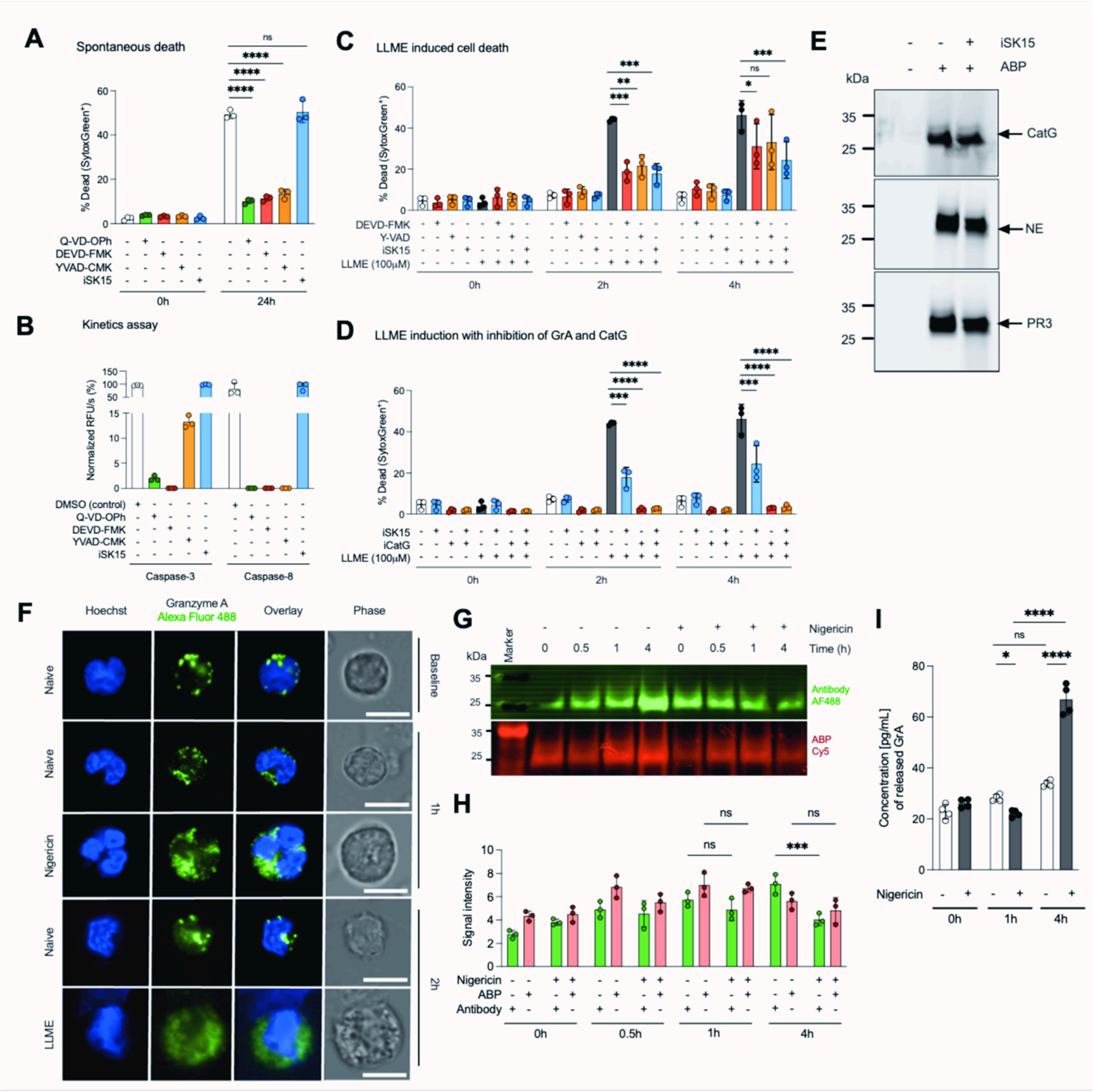


Figure 4

GrA inhibition selectively rescues pyroptotic but not apoptotic neutrophil death, and GrA is retained within the neutrophil during nigericin-induced pyroptosis until its release in the latest phase of the process.

(A) Spontaneous neutrophil death assessed at 0 and 24 h. Freshly isolated neutrophils were pre-treated with 50 µM QVD-OPh, 20 µM DEVD-FMK, 20 µM YVAD-CMK, or 500 nM iSK15 prior to culture without additional stimulation. **(B)** Evaluation of caspase-3 and caspase-8 inhibition using iSK15 and reference

caspase inhibitors. Recombinant and purified Casp-3 and Casp-8 were pre-treated for 1 h with 500 nM iSK15, 20 μM DEVD-FMK, 20 μM YVAD-CMK, or 50 μM Q-VD-OPh, following appropriate substrate (see methods section). **(C)**LLME-induced cell death. Neutrophils pre-treated for 1 h with 500 nM iSK15, 20 μM DEVD-FMK, 20 μM YVAD-CMK, or 50 μM Q-VD-OPh were stimulated with 100 μM LLME and assessed at 0, 2, and 4 h. Cell death in all panels was assessed by flow cytometry as the percentage of SYTOX Green-positive cells. **(D)** LLME-induced cell death. Neutrophils pre-treated for 1 h with 500 nM iSK15, 20 μM DEVD-FMK, 20 μM YVAD-CMK, or 50 μM Q-VD-OPh were stimulated with 100 μM LLME and assessed at 0, 2, and 4 h. Cell death in all panels was assessed by flow cytometry as the percentage of SYTOX Green-positive cells. **(E)** Gel electrophoresis of ABP for CatG, NE and PR3 used on human neutrophil lysates, to verify the selectivity of iSK15 on GrA. Lysates were pre-treated with iSK15. Data represent mean ± SD from n = 3 independent experiments. **(F)** Confocal images representing GrA redistribution during nigericin and LLME induction. Images represent nucleus counterstained with Hoechst, GrA with Alexa Fluor 488 antibody, and overlay and phase. Scale bars; 10 μm **(G)** Western blot of GrA protein (anti-GrA antibody, AlexaFluor 488, green) and GrA activity (SK15.5 ABP, Cy5, red) in lysates of neutrophils stimulated with 10 μM nigericin or left untreated, collected at 0, 30, 60, and 240 min. **(H)** Densitometry of GrA antibody signal and ABP signal from (B). **(I)** GrA concentration in culture supernatants of neutrophils stimulated with 10 μM nigericin for 1 or 4 h, measured by ELISA. Bars represent mean ± SD; individual data points represent n = 3 independent experiments each performed on neutrophils from a different healthy donor. Statistical comparisons by two-way ANOVA with Šídák's multiple comparisons test; ns, not significant; *$p < 0.05$; **$p < 0.01$; ***$p < 0.001$; ****$p < 0.0001$.

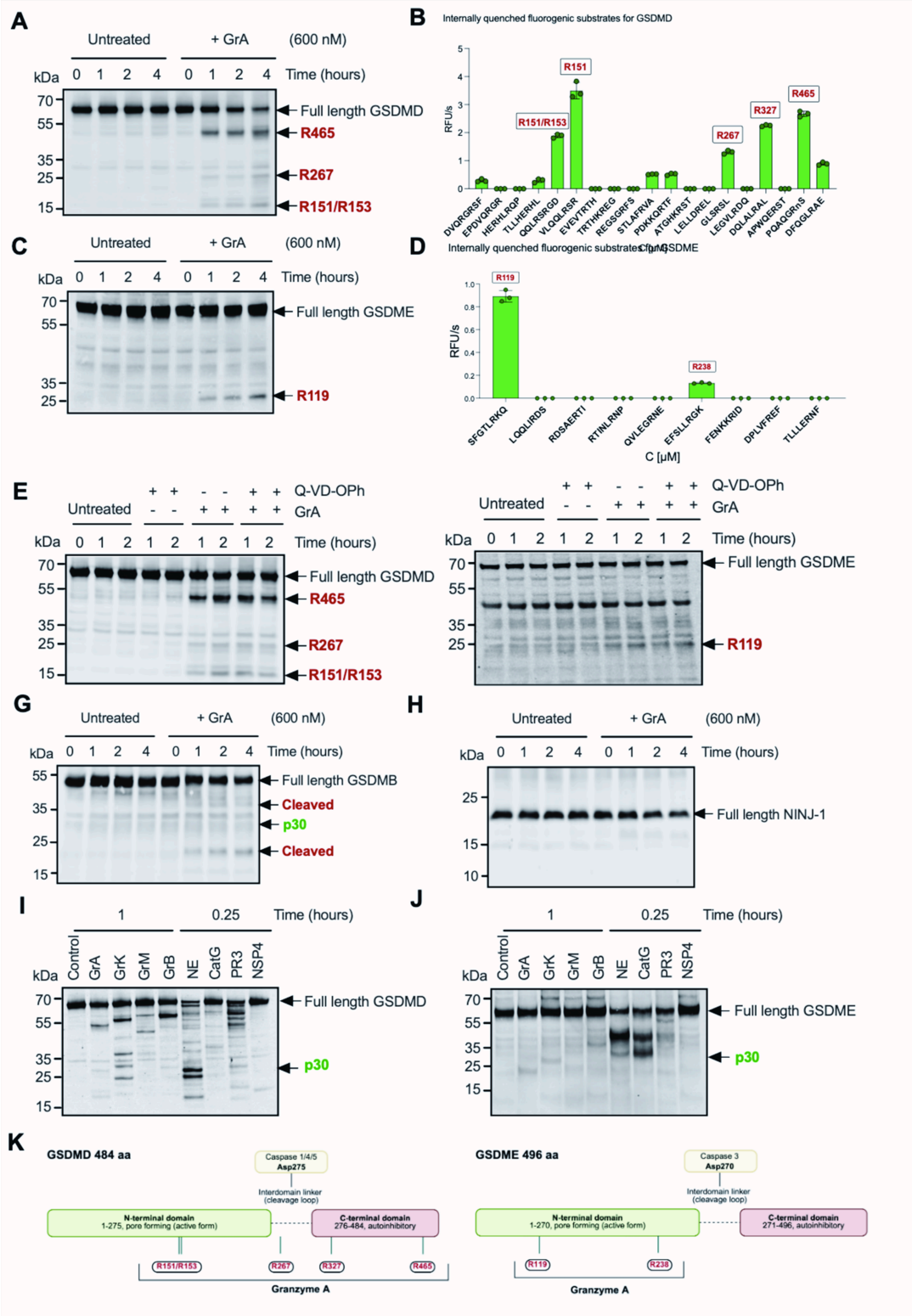


Figure 5

GrA directly cleaves GSDMD and GSDME but not NINJ1 and displays distinct substrate specificity compared with other neutrophil serine proteases.

(A)*Time-course analysis of GrA-mediated cleavage of GSDMD. HEK293T cell lysates overexpressing the indicated proteins were incubated with 600 nM GrA for 0, 1, 2 or 4 h. Control lysates were incubated for the corresponding time periods in the absence of GrA.* ***(B)*** *Kinetic analysis of internally quenched fluorogenic*

substrates for GSDMD cleaved by GrA. ***(C)*** *Time-course analysis of GrA-mediated cleavage of GSDME. HeLa cell lysates overexpressing the indicated proteins were incubated with 600 nM GrA for 0, 1, 2 or 4 h. Control lysates were incubated for the corresponding time periods in the absence of GrA.* ***(D)*** *Kinetic analysis of internally quenched fluorogenic substrates for GSDME, cleaved by GrA.* ***(E, F)*** *Effect of caspase inhibition on GrA-mediated cleavage of GSDMD (E) and GSDME (F). HeLa lysates overexpressing GSDMD or GSDME were pre-incubated with the pan-caspase inhibitor Q-VD-OPh for 1 h before addition of GrA. Lysates were then incubated with GrA for 1 or 2 h, while control samples were incubated in parallel without GrA for the corresponding time periods.* ***(G, H)*** *Time-course analysis of GrA-mediated cleavage of GSDMB (G) and NINJ-1 (H). HeLa cell lysates overexpressing the indicated proteins were incubated with 600 nM GrA for 0, 1, 2 or 4 h. Control lysates were incubated for the corresponding time periods in the absence of GrA.* ***(I, J)*** *Cleavage of GSDMD (I) and GSDME (J) by granzymes and NSPs. HEK293T lysates overexpressing GSDMD and HeLa lysates overexpressing GSDME were incubated with granzymes (600 nM, 1 h) or other NSPs (100 nM, 15 min).* ***(K)*** *Schematic representation of potential cleavage sites of GSDMD and GSDME by GrA in the N- and C-terminal domains compared to activation sites by caspases.*

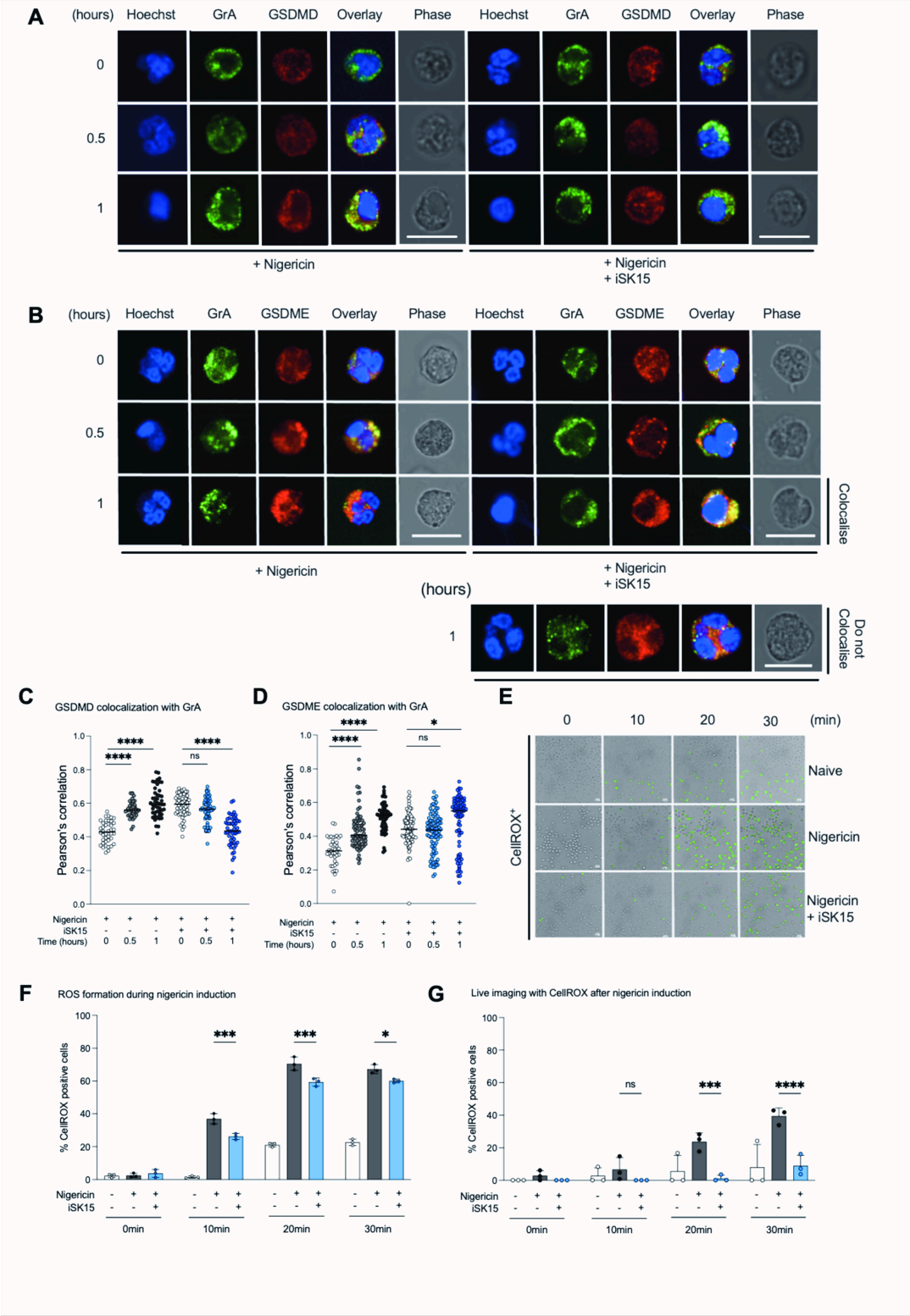


Figure 6

GrA colocalization with GSDME during nigericin induction and ROS generation. **(A, B)** Confocal images representing colocalization of GSDMD (A) and GSDME (B) with GrA. Freshly isolated human neutrophils pre-treated ± 500 nM iSK15 and stimulated with 10 µM nigericin for 0, 30, or 60 min prior to fixation and immunofluorescence staining. Scale bar, 10 µm. Both populations at 60 min, that represent two distinct populations labelled as: colocalise and do not colocalise. **(C, D)** Pearson's correlation coefficients

quantifying colocalization of GrA with GSDMD (C) and GSDME (D) in freshly isolated human neutrophils pre-treated ± 500 nM iSK15 and stimulated with 10 µM nigericin for 0, 30, or 60 min. Each data point represents one cell; n > 100 cells per condition from 3 independent experiments. **(E)** Representative confocal live-cell images of freshly isolated neutrophils pre-treated ± 500 nM iSK15 and stimulated with 10 µM nigericin. CellROX (5 µM) was added at the start of imaging to detect ROS production. Images acquired at T = 0, 10, 20 and 30 min. Scale bar, 10 µm. **(F)** Flow cytometry quantification of CellROX-positive cells at 0, 10, 20, and 30 min post-nigericin stimulation ± 500 nM iSK15. **(G)** Quantification of CellROX-positive as percentage of total cells over 120 min from live imaging in (E). Bars represent mean ± SD; n = 3 independent experiments from different healthy donors. Statistical comparisons by two-way ANOVA with Šídák's multiple comparisons test; ns, not significant; *$p < 0.05$; **$p < 0.01$; ***p < 0.001; ****p < 0.0001.

Supplementary Files

This is a list of supplementary files associated with this preprint. Click to download.

- CDDTable1PK.xlsx
- 260826GrApaperSuppl.1FullsizeWB.docx
- 260826GrApaperSupplementaryFile2.docx
- Supplementarytable1.docx